Stem Cell Reports
Article

OPEN ACCESS

p38α MAPK Regulates Lineage Commitment and OPG Synthesis of Bone Marrow Stromal Cells to Prevent Bone Loss under Physiological and Pathological Conditions

Qian Cong,[1,8] Hao Jia,[1,2,8] Soma Biswas,[1] Ping Li,[1] Shoutao Qiu,[1] Qi Deng,[1] Xizhi Guo,[1] Gang Ma,[1] Jenny Fang Ling Chau,[3] Yibin Wang,[4] Zhen-Lin Zhang,[5] Xinquan Jiang,[6] Huijuan Liu,[1,*] and Baojie Li[1,7,*]

[1]Key Laboratory for the Genetics of Developmental and Neuropsychiatric Disorders, Bio-X Institutes, Ministry of Education, Shanghai Jiao Tong University, Shanghai 200240, China

[2]Faculty of Basic Medicine, Department of Biochemistry and Molecular Cell Biology, Shanghai Jiao Tong University, School of Medicine, Shanghai 200025, China

[3]The Institute of Molecular and Cell Biology, Singapore 138673, Singapore

[4]Division of Molecular Medicine, Departments of Anesthesiology, Medicine and Physiology, Molecular Biology Institute, Cardiovascular Research Laboratories, David Geffen School of Medicine, Los Angeles, CA 90095, USA

[5]Department of Orthopedic Surgery, Shanghai Jiao Tong University affiliated the Sixth People's Hospital, Shanghai 200233, China

[6]Department of Prosthodontics, Oral Bioengineering and Regenerative Medicine Lab, Shanghai Research Institute of Stomatology, Ninth People's Hospital affiliated to Shanghai Jiao Tong University, School of Medicine, Shanghai 200011, China

[7]Translational Medical Center for Stem Cell Therapy, Shanghai East Hospital, Tongji University School of Medicine, Shanghai 200120, China

[8]Co-first author

*Correspondence: liuhj@sjtu.edu.cn (H.L.), libj@sjtu.edu.cn (B.L.)

http://dx.doi.org/10.1016/j.stemcr.2016.02.001

SUMMARY

Bone marrow-derived mesenchymal stromal cells (BM-MSCs) are capable of differentiating into osteoblasts, chondrocytes, and adipocytes. Skewed differentiation of BM-MSCs contributes to the pathogenesis of osteoporosis. Yet how BM-MSC lineage commitment is regulated remains unclear. We show that ablation of *p38α* in *Prx1*+ BM-MSCs produced osteoporotic phenotypes, growth plate defects, and increased bone marrow fat, secondary to biased BM-MSC differentiation from osteoblast/chondrocyte to adipocyte and increased osteoclastogenesis and bone resorption. p38α regulates BM-MSC osteogenic commitment through TAK1-NF-κB signaling and osteoclastogenesis through osteoprotegerin (OPG) production by BM-MSCs. Estrogen activates p38α to maintain OPG expression in BM-MSCs to preserve the bone. Ablation of *p38α* in BM-MSCs positive for *Dermo1*, a later BM-MSC marker, only affected osteogenic differentiation. Thus, p38α mitogen-activated protein kinase (MAPK) in *Prx1*+ BM-MSCs acts to preserve the bone by promoting osteogenic lineage commitment and sustaining OPG production. This study thus unravels previously unidentified roles for p38α MAPK in skeletal development and bone remodeling.

INTRODUCTION

Bone marrow-derived mesenchymal stromal cell (BM-MSC)-derived osteoblasts and chondrocytes are responsible for bone and cartilage modeling/remodeling, respectively (Harada and Rodan, 2003; Wu et al., 2009). Osteoblasts are defined by lineage-specific transcription factors RUNX2 and OSTERIX, whereas chondrocytes are defined by SOX9 (Karsenty, 2008; Long, 2012). In addition, BM-MSCs are capable of differentiating into adipocytes, which are defined by C/EBPα and PPARγ. Under certain conditions, e.g., aging, the lineage differentiation potentials of BM-MSCs are altered. Aged BM-MSCs tend to differentiate into adipocytes at the cost of osteoblasts, which contributes to the pathogenesis of senile osteoporosis and yellowing of the bone marrow (Baldridge et al., 2010; Rachner et al., 2011). Reversal of the biased differentiation of aged BM-MSCs is a strategy employed for the prevention/treatment of osteoporosis (Berendsen and Olsen, 2014; Kassem and Marie, 2011; Lecka-Czernik and Stechschulte, 2014; Zaidi et al., 2012). However, how BM-MSC lineage commitment is regulated remains less well understood.

Osteoblast-mediated bone formation is balanced by osteoclast-mediated bone resorption. Osteoclasts are derived from hematopoietic stem cell-derived monocytes, which are defined by transcription factors including PU.1, NF-κB, and NFATc1 (Edwards and Mundy, 2011). Under normal conditions, bone formation and resorption are coordinated via complex coupling mechanisms. Some of the osteogenic regulators, e.g., transforming growth factor β1 (TGFβ1), bone morphogenetic proteins (BMPs), and insulin growth factor-1 (IGF-1), are synthesized by osteoclasts or released from bone matrix during resorption (Crane and Cao, 2014; Engin and Lee, 2010; Guihard et al., 2012; Henriksen et al., 2014; Pederson et al., 2008; Takeshita et al., 2013), whereas the master regulators of osteoclast differentiation, macrophage colony stimulating factor (M-CSF), receptor activator of nuclear factor-kappaB ligand (RANKL), and osteoprotegerin (OPG), are believed

to be produced by osteoblasts, especially osteocytes (Edwards and Mundy, 2011; Karsenty, 2008; Kearns et al., 2008; Lacey et al., 2012; Lian et al., 2011). Disruption of bone formation-resorption coupling underlies the etiology of osteoporosis (Hofbauer et al., 1999; Michael et al., 2005).

p38 mitogen-activated protein kinases (MAPKs) are activated by stress, cytokines, and growth factors, some of which are involved in bone development and remodeling, e.g., TGFβ1 and BMPs (Cuadrado and Nebreda, 2010; Han and Sun, 2007; Sorrentino et al., 2008; Yamashita et al., 2008). p38 MAPKs phosphorylate a number of transcription factors such as C/EBPα, MEF2, RUNX2, SOX9, and p53 to regulate the expression of many target genes and subsequently cell proliferation, differentiation, and apoptosis (Greenblatt et al., 2013; Thouverey and Caverzasio, 2015a). Ablation of *p38β* or *p38α* in osteoprogenitors or osteoblasts revealed that p38 MAPKs play positive roles in osteoblast maturation, via phosphorylating RUNX2/OSX, without affecting osteoclastogenesis or bone resorption via the coupling mechanisms (Greenblatt et al., 2010, 2013; Rodriguez-Carballo et al., 2014; Thouverey and Caverzasio, 2012). Ablation of *p38α* or constitutive activation of p38 MAPKs in differentiated chondrocytes inhibits their differentiation (Hutchison, 2013; Oh et al., 2000; Stanton et al., 2004; Zhang et al., 2006). Yet it is still unknown whether p38α plays a role in the stem cells for osteoblasts and chondrocytes, including their self-renewal and cell fate determination. Unlike the differentiated cells, the multipotent BM-MSCs in general do not express lineage-specific transcription factors such as RUNX2 or SOX9, the phosphorylation targets of p38 MAPKs (Greenblatt et al., 2013; Thouverey and Caverzasio, 2015a). Thus, p38 MAPK may employ other mechanisms to decide the fates of BM-MSCs.

Here we ablated *p38α*, the essential *p38* isoform, in BM-MSCs using *Prx1-Cre* and *Dermo1-Cre* mouse lines, respectively, and found that while both *Prx1-Cre; p38α$^{f/f}$* mice and *Dermo1-Cre; p38α$^{f/f}$* mice developed osteoporosis, *Prx1-Cre; p38α$^{f/f}$* mice also showed alterations in growth plate and bone marrow fat. Further studies revealed that p38α plays a role in self-renewal and lineage determination of *Prx1*+ BM-MSCs. Moreover, *Prx1-Cre; p38α$^{f/f}$* mice, but not *Dermo1-Cre; p38α$^{f/f}$* mice, showed increased osteoclastogenesis and bone resorption. p38α was found to control OPG production in *Prx1*+ BM-MSCs under normal conditions or in response to estrogen. *Prx1-Cre; p38α$^{f/f}$* mice were resistant to ovariectomy-induced bone loss. This study thus reveals that p38α expressed in *Prx1*+ cells regulates BM-MSC cell fate decision in a cell-autonomous manner and osteoclastogenesis via controlling production of OPG.

RESULTS

Ablation of *p38α* in *Prx1*+ BM-MSCs Leads to Osteoporosis and Cartilage Anomaly

To study the functions of p38α in BM-MSCs, we ablated *p38α* with a *Prx1-Cre* mouse line, which has been used to delete genes of interest in BM-MSCs (Greenbaum et al., 2013; Logan et al., 2002). Although inconsistent results have been reported regarding the in vivo multipotency of *Prx1*+ BM-MSCs, our lineage-tracing experiments using *Prx1-Cre; Rosa-tdTomato* and *Rosa-LacZ* mice confirmed that *Prx1* could label osteoblasts, chondrocytes, and bone marrow adipocytes in vivo (Figure S1A). Immuno-staining of *Prx1-Cre; p38α$^{f/f}$* mouse tissues revealed a great reduction of active p38 MAPKs in osteoblasts and chondrocyte of the bones, but not in skeletal muscle or heart (Figure S1B). The mutant mice were born at the expected Mendelian frequency with normal body weight, yet older mice showed a modest shortening of the hind limbs (Figures S1C and S1D). Histological analysis revealed that *p38α* deletion in *Prx1*+ BM-MSCs resulted in a decrease in trabecular bone volume and mineralization (Figure 1A). Histomorphometry analysis and micro-computed tomography (CT) analysis also revealed a decrease in trabecular volume and number, and an increase in trabecular separation (Table 1 and Figure 1B). The growth plates were thinner in *Prx1-Cre; p38α$^{f/f}$* mice than in control mice (Figures 1A and 1C), with a decrease in the number of hypertrophic chondrocytes (Figure 1C). This may contribute to the short limb phenotype of the mutant mice. In addition, the mutant mice showed an increase in bone marrow fat (Figures 1D and 1E). These results show that ablation of *p38α* in *Prx1*+ BM-MSC and its progenies affects bone mass, cartilage and growth plate, and bone marrow fat, validating the multipotency of *Prx1*+ BM-MSCs.

Ablation of *p38α* in *Dermo1*+ BM-MSCs Leads to Osteoporosis but Not Cartilage Anomaly

In addition to *Prx1*, *Dermo1* has been implicated as a BM-MSC (or mesenchymal progenitor) marker downstream of *Prx1*, and the *Dermo1-Cre* mouse has been used to generate BM-MSC-specific gene knockout mouse lines as well (Qin et al., 2015; Tran et al., 2010). Previous studies showed that bone marrow contains similar numbers of *Prx1*+ cells and *Dermo1*+ cells (Greenbaum et al., 2013; Logan et al., 2002; Yu et al., 2003). We then ablated *p38α* using a *Dermo1-Cre* knockin mouse line (Logan et al., 2002). Surprisingly, *Dermo1-Cre; p38α$^{f/f}$* mice did not show a significant defect in growth plate or bone marrow fat (Figure S1E and data not shown), although they showed an osteoporotic phenotype (Table S1). These results suggest that *Dermo1*+ BM-MSCs may have limited chondrogenesis

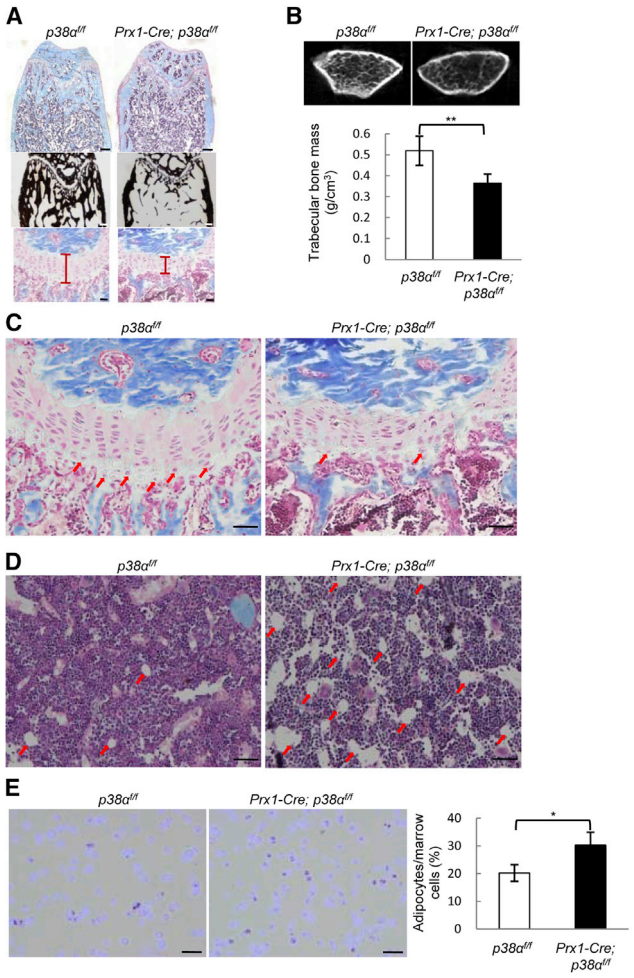

Figure 1. Deletion of *p38α* in *Prx1*+ BM-MSCs Led to Osteoporosis and Growth Plate Defects

(A) Representative images of H&E and Von Kossa staining of the femur bones of 10-week-old *Prx1-Cre; p38α$^{f/f}$* and control mice to show trabecular bones (upper panel, scale bar, 200 μm), bone mineralization (middle panel, scale bar, 200 μm), and growth plate (lower panel, scale bar, 50 μm).

(B) Micro-CT results confirmed that *Prx1-Cre; p38α$^{f/f}$* mice showed a decrease in bone mass. Bottom panel: quantitation data. Data represent means ± SEM of eight independent experiments, **p < 0.01.

(C) The growth plates at a higher magnification. Arrows indicate hypertrophic chondrocytes. Scale bar, 50 μm.

(D) The *Prx1-Cre; p38α$^{f/f}$* mice showed an increase in bone marrow fat. *p38α* deficiency led to an increase in bone marrow adipocytes in 8-month-old mice. Arrows indicate the adipocytes in H&E staining. Scale bar, 50 μm.

(E) The bone marrow smear assay also revealed an increase in bone marrow fat cells in the mutant mice. Right panel: quantitation data. Scale bar, 20 μm. Data represent means ± SEM of three independent experiments. *p < 0.05.

See also Figure S1.

potential, thus representing a less primitive BM-MSC population than *Prx1*+ BM-MSCs.

p38α Controls Proliferation and Multi-Lineage Differentiation of *Prx1*+ BM-MSCs

We found that bone formation rates, bone mineralization rates, and the numbers of osteoblasts were all decreased in *Prx1-Cre; p38α$^{f/f}$* mice (Table 1). However, *p38α* deficiency led to an increase in the number of bone marrow alkaline phosphatase (ALP)-positive colony-forming units (Figure 2A), an indication of the number of BM-MSCs. This was likely caused by enhanced BM-MSC proliferation, as ablation of *p38α* led to an increase in proliferation rate and KI67-positive cells in BM-MSC cultures (Figures 2B and 2C, and S2A), which was associated with a decrease in the levels of p53, p21, and p16 (Figure 2C), negative regulators of cell proliferation that have been shown to be regulated by p38 MAPKs (Wagner and Nebreda, 2009). *p38α−/−* bone sections also showed an increase (1.79 ± 0.39 fold, n = 3) in the number of KI67-positive cells, including marrow cells (Figure 2D). However, *p38α* deficiency did not affect the apoptosis rates of BM-MSCs or on bone sections (Figures S2B and S2C).

We then tested the differentiation potentials of *p38α−/−* BM-MSCs and found that *Prx1*+ BM-MSCs deficient for *p38α* showed decreased osteogenic differentiation, manifested by a decrease in ALP staining, mineralization, and expression of osteoblast-specific markers such as *Runx2*, *Osx*, *Fra-1*, *Atf4*, *Col1α*, and osteocalcin (Figures 2E and 2F, and S2D). The mutant cells also showed decreased chondrocyte differentiation (Figure 2E), accompanied by a decrease in *Sox9* expression (Figure 2F). The growth plate phenotype appears to be more severe than that in mice with *p38α* ablated in differentiated chondrocytes (Hutchison, 2013). However, the mutant cells showed enhanced adipocyte differentiation (Figure 2E), accompanied by an increase in *Pparγ* and *C/ebpα* expression (Figure 2F). Taken together, these results suggest that *p38α* deficiency alters the multi-lineage differentiation potentials of *Prx1*+ BM-MSCs, consistent with thinning of growth plate (Figures 1A and 1C), and an increase in bone marrow adipocytes observed in *Prx1-Cre; p38α$^{f/f}$* mice (Figures 1D and 1E).

p38α Regulates BM-MSC Osteogenic Commitment via TAK1-NF-κB Signaling

Previous studies have shown that p38 MAPKs can promote osteoblast differentiation by phosphorylating RUNX2/OSX. Our study and those of others also showed that p38 MAPKs were required for *Osx* expression (Hu et al., 2003; Ortuno et al., 2013; Phimphilai et al., 2006; Wang et al., 2007). Yet *Runx2* and *Osx* are expressed in osteoprogenitors and osteoblasts but rarely in multipotent BM-MSCs (Figure 3A). Instead, we found that *p38α−/−* BM-MSCs showed

Table 1. Histomorphometry Parameters of *Prx1-Cre; p38α$^{f/f}$* and Control Mice, Ovariectomized *Prx1-Cre; p38α$^{f/f}$* and Control Mice

	p38α$^{f/f}$	*Prx1-Cre; p38α$^{f/f}$*	*p38α$^{f/f}$ OVX*	*Prx1-Cre; p38α$^{f/f}$ OVX*
BV/TV (%)	22.914 ± 5.66	10.336 ± 5.79**	15.552 ± 2.76**	12.017 ± 3.99
Tb.Ar (%)	19.711 ± 4.90	5.827 ± 2.78**	12.241 ± 2.09**	8.238 ± 2.36
Tb.Th (μm)	36.669 ± 2.86	18.766 ± 3.13**	26.768 ± 2.88**	20.713 ± 4.52
Tb.Sp (μm)	193.124 ± 30.73	540.127 ± 211.85*	355.784 ± 41.12**	448.729 ± 28.23
Tb.N (no./mm)	5.950 ± 0.76	2.70 ± 1.51**	3.646 ± 0.33**	2.769 ± 0.41
MAR (μm/d)	1.749 ± 0.168	1.243 ± 0.097**	1.768 ± 0.096	1.240 ± 0.188
BFR (μm/d)	75.880 ± 3.896	56.437 ± 4.58**	71.771 ± 3.88	55.970 ± 6.1
OB.S/BS (%)	17.016 ± 1.096	11.600 ± 1.68**	16.001 ± 1.00	11.933 ± 0.95

Data represent means ± SEM of eight independent experiments, **p < 0.01, *p < 0.05 when the value of mutant or ovariectomized mice was compared with that of control mice.
See also Table S1.

enhanced activation of the TAK1-NF-κB pathway (Figure 3B), which has been recently shown to inhibit BM-MSC osteogenic differentiation (Chang et al., 2009; Yao et al., 2014; Yu et al., 2014). p38 MAPKs have been shown to phosphorylate TAB1/2 to inhibit TAK1 activation in several cell types (Cheung et al., 2003; Wagner and Nebreda, 2009). We found that inhibition of TAK1 with 5Z-7-oxozeaenol or inhibition of NF-κB with BAY11-7082, reversed the osteogenic differentiation defects of *p38α−/−* BM-MSCs, manifested by the decrease in ALP staining, mineralization staining, and expression of osteoblast markers (Figures S3A–S3C), although the effects of the inhibitors on osteogenic differentiation of wild-type (WT) BM-MSCs were rather modest. These findings were confirmed by knockdown of *Tak1* or *Nf-κB (p65)* with siRNA in *p38α−/−* BM-MSCs (Figures 3C and 3D). These results suggest that p38α can regulate osteogenic differentiation of *Prx1+* BM-MSCs via the TAK1-NF-κB pathway. At the later stages of osteoblastogenesis, p38 MAPK may act on RUNX2 and OSTERIX to further promote osteoblast differentiation.

Ablation of *p38α* in BM-MSC Promotes Osteoclastogenesis In Vivo and In Vitro

We noticed that in *Prx1-Cre; p38α$^{f/f}$* mice, the extent of the decrease in bone mass (down to 45.4% of the control) exceeds that of the decrease in bone formation rates (down to 74.3% of the control) (Table 1), suggesting that bone resorption may contribute to the osteoporotic phenotype as well. Indeed, we found that *Prx1-Cre; p38α$^{f/f}$* mice showed an increase in osteoclast surface, the number of osteoclasts (Figures 4A and 4B), and the levels of urine deoxypyridinoline (DPD), an in vivo bone resorption marker (Figure 4C), suggesting that ablation of *p38α* in *Prx1+* BM-MSCs promoted osteoclastogenesis and bone resorption in a non-cell-autonomous way. This activity of p38α appears to be unique to *Prx1+*BM-MSCs as previous studies have reported that ablation of *p38α* or *p38β* in osteoprogenitors or osteoblasts did not affect osteoclastogenesis or bone resorption (Greenblatt et al., 2010; Rodriguez-Carballo et al., 2014; Thouverey and Caverzasio, 2012). We found that ablation of *p38α* in *Dermo1+* cells did not significantly alter the number of osteoclasts or bone resorption rate (Figure S1F). These results, together with our observation that *Dermo1+* cells have minimal chondrogenic activity, suggest that p38α plays an important role in BM-MSC-osteoclastogenesis coupling, but not in osteoprogenitor/osteoblast communication to osteoclastogenesis.

We also found that in co-culture experiments, BM-MSCs were able to support osteoclastogenesis and more importantly, *p38α−/−* BM-MSCs showed a heightened ability in promoting osteoclastogenesis (Figure 4D). Similarly, the *p38α−/−* BM-MSC culture medium was more capable of promoting osteoclast differentiation than the WT BM-MSC culture medium (Figure 4E). These results suggest that *p38α* deficiency might affect the synthesis of RANKL, M-CSF, OPG, or other molecules that are involved in regulation of osteoclastogenesis. The finding that ablation of *p38α* in BM-MSCs but not in osteoblasts affects osteoclastogenesis may be explained by differential expression of RANKL, OPG, or M-CSF in BM-MSCs and osteoblasts. Yet qPCR assays revealed that these two cell types expressed similar levels of *Rankl*, *Opg*, and *M-csf* at the mRNA levels (Figure S4).

p38α Regulates the Expression of *Opg* via CREB in *Prx1+* BM-MSCs

We found that *p38α* deficiency led to a 4-fold decrease in the mRNA levels of *Opg* (Figure 5A), and a modest increase in mRNA levels of *M-csf* and *Rankl* (Figure 5A). A decrease in *Opg* mRNA levels and a modest increase in *Rankl* and *M-csf* levels were also observed in the bone extracts of *Prx1-Cre;*

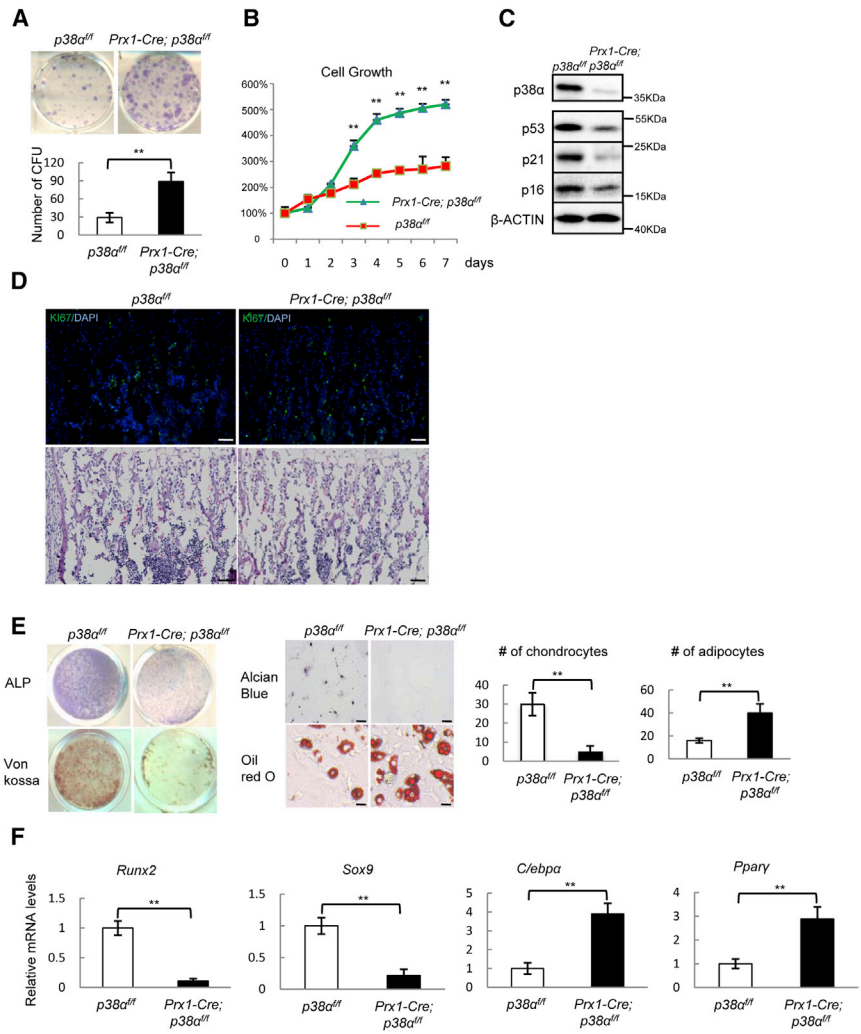

Figure 2. *p38α* Ablation Enhanced Proliferation of *Prx1*+ BM-MSCs and Resulted in Skewed BM-MSC Tri-lineage Differentiation

(A) *Prx1-Cre; p38α*$^{f/f}$ mice showed an increase in the number of ALP-positive colony-forming units. A total of 5 × 10^6 cells/well was plated onto six-well plates, which were stained for ALP after 7 days in culture. Bottom panel: quantitation data. Data represent means ± SEM of three independent experiments, **p < 0.01.

(B) *p38α−/−* BM-MSC showed increased proliferation. WT and *Prx1-Cre; p38α*$^{f/f}$ BM-MSCs were cultured in BM-MSC culture medium and cells were counted at different time. Data represent means ± SEM of three independent experiments, **p < 0.01.

(C) Ablation of *p38α* in BM-MSC showed a decrease in p38α, p16, p53, and p21 protein levels compared with control cells. The BM-MSCs were isolated from WT and *Prx1-Cre; p38α*$^{f/f}$ mice, cultured in BM-MSC culture medium to log phase, and were then collected. The protein levels of these genes were analyzed by western blot.

(D) *p38α−/−* bone sections also showed an increase in the number of KI67-positive cells. Scale bar, 100 μm.

(E) *p38α−/−* BM-MSC showed an alteration in differentiating into the three lineages. WT and *p38α−/−* BM-MSCs were cultured in differentiation medium for osteoblasts, chondrocytes, or adipocytes for different periods of time and then stained for ALP, mineralization, Alcian blue (scale bar, 100 μm), or oil red O (scale bar, 20 μm). Right panel: quantitation data to show the numbers of chondrocytes and adipocytes per well. Data represent means ± SEM of three independent experiments, **p < 0.01.

(F) *p38α−/−* BM-MSCs showed an alteration in the expression of lineage-specific transcription factors and functional molecules. The cells were cultured as described in Figure 3E, from which total RNA was isolated. qPCR was used to determine the mRNA levels of these genes. Data represent means ± SEM of three independent experiments, **p < 0.01.

See also Figure S2.

p38α$^{f/f}$ mice (Figure 5B). In co-culture experiments, supplementing the *p38α−/−* BM-MSC-monocytes co-culture with OPG could inhibit osteoclast differentiation (Figure 5C). These results suggest that *p38α−/−* BM-MSC may promote osteoclastogenesis by down-regulating OPG.

It is likely that p38α controls *Opg* transcription via its downstream transcription factors. Screening of these transcription factors with siRNA revealed that *Creb* may be involved (data not shown). We found that *p38α* deficiency led to a decrease in CREB phosphorylation on Ser133 and moreover, knockdown of *Creb* with siRNA significantly decreased the mRNA levels of *Opg* in normal BM-MSCs (Figures 5D and 5E), suggesting that CREB is required for expression of OPG in BM-MSCs. Chromatin-immunoprecipitation (ChIP) assays revealed that two CREB binding sites exist in the promoter of *Opg* gene (Figure 5F). Taken together, our results showed that *Opg* transcription in BM-MSCs is regulated by the p38α-CREB axis and that *Opg* is a target gene of CREB.

Prx1-Cre; p38α$^{f/f}$ Mice Are Resistant to Estrogen Deficiency-Induced Bone Loss

The above studies revealed that the p38α-CREB-OPG axis in BM-MSCs regulates osteoclastogenesis. One of the

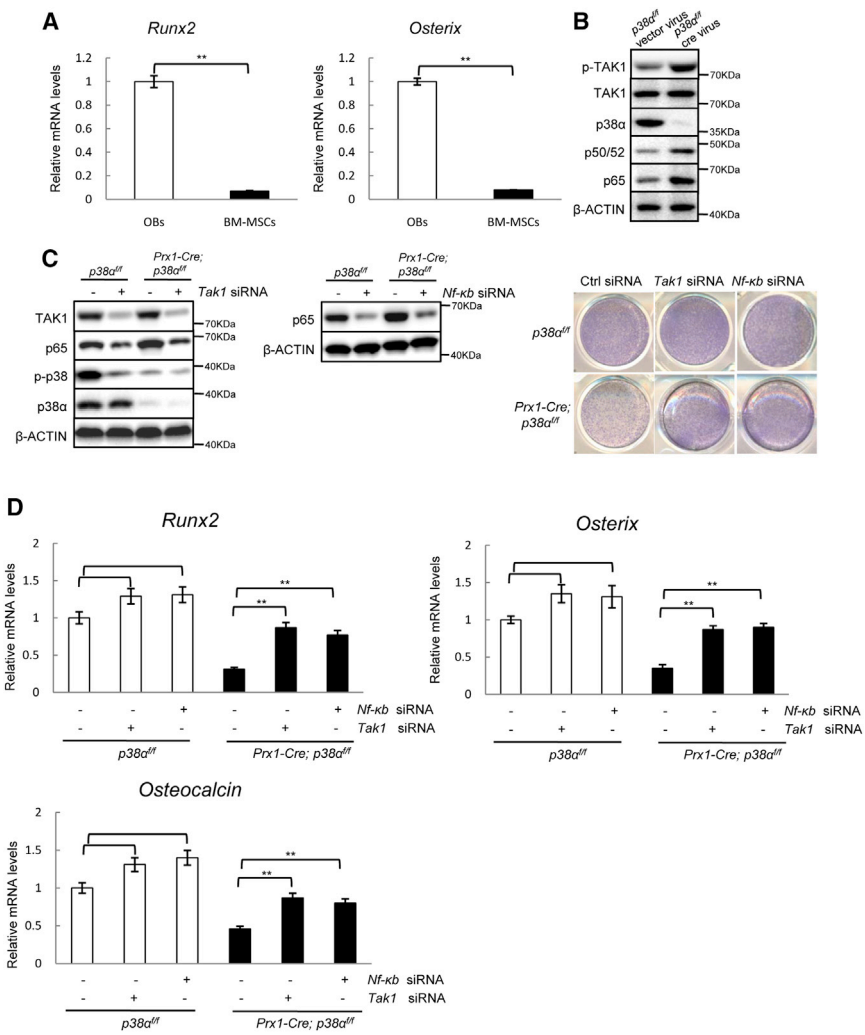

Figure 3. p38α Regulated BM-MSC Osteogenic Differentiation via TAK1-NF-κB Signaling

(A) *p38α−/−* and WT BM-MSCs showed minimal expression of *Runx2* and *Osx*. Data represent means ± SEM of three independent experiments, **p < 0.01.

(B) *p38α−/−* BM-MSCs showed enhanced TAK1-NF-κB signaling. BM-MSCs were isolated from $p38\alpha^{f/f}$ mice and cultured in BM-MSC medium, infected with Cre-expressing retrovirus or empty retrovirus, selected against puromycin, and then collected. The activation and protein levels of TAK1, NF-κB, and p38α were determined by western blot analysis.

(C) Knockdown of *Tak1* or *Nf-κb p65* with siRNA rescued the osteogenic differentiation defect of *p38α−/−* BM-MSCs. WT and *p38α−/−* BM-MSCs were transfected with control, *Tak1*, or *Nf-κb* siRNA for 2 days and then cultured in osteoblast differentiation medium for 4 more days. The cells were stained for ALP (right panel). Left panel: western blot results of knockdown of TAK1 or NF-κB.

(D) qPCR results showed that knockdown of *Tak1* or *Nf-κb p65* with siRNA rescued the osteogenic differentiation defect of *p38α−/−* BM-MSCs. Data represent means ± SEM of three independent experiments, **p < 0.01.

See also Figure S3.

pathological conditions that involves osteoblast-osteoclast interaction is estrogen deficiency-induced osteoporosis, which affects more than 50% of women over 50 years of age (Manolagas et al., 2013; Rachner et al., 2011). We found that estradiol activated p38 MAPKs in a time- and dose-dependent manner in BM-MSCs (Figures 6A and 6B), and ovariectomy led to a decrease in p38 MAPKs activation on bone sections, in particular the osteoblast-like cells aligning the trabecular bone surface (Figure 6C), suggesting that p38α MAPK is a nongenomic signaling molecule of estrogen. Moreover, we found that *p38α* deficiency down-regulated the mRNA and protein levels of estrogen receptor α (ERα) but not ERβ in BM-MSCs and osteoblasts (Figures S5A and S5B), suggesting that p38α is required for optimal expression of ERα in these cells.

Furthermore, estradiol promoted *Opg* expression in WT BM-MSCs but not in *p38α−/−* BM-MSCs, suggesting a necessary role for p38α in estrogen-induced *Opg* expression (Figure 6D). Moreover, *p38α−/−* osteoblasts were not responsive to estradiol-induced *Opg* expression (Figure S5C). In addition to inhibiting p38 MAPK activation, ovariectomy also down-regulated *Opg* expression in the bone of WT mice. The basal levels of *Opg* in the bones of *Prx1-Cre; p38α*$^{f/f}$ mice were low, which could not be further down-regulated by ovariectomy (Figure 6E). These results suggest that estrogen may induce OPG expression via p38α in BM-MSCs and osteoblasts to suppress osteoclastogenesis. If this p38α-controlled OPG production plays a role in the bone-sparing effects of estrogen, ovariectomy would not further affect osteoclastogenesis or bone resorption in *Prx1-Cre; p38*$^{f/f}$ mice due to low levels of OPG. We ovariectomized *Prx1-Cre; p38α*$^{f/f}$ and control mice and waited for 4 weeks before analyzing the bone parameters, and found that ovariectomy led to a decrease in bone mass in normal mice, which is accompanied by an increase in the number of osteoclasts and bone resorption rate (Table 1; Figures 6F and 6G), yet ovariectomy did not further reduce the bone mass in *Prx1+* BM-MSC-specific

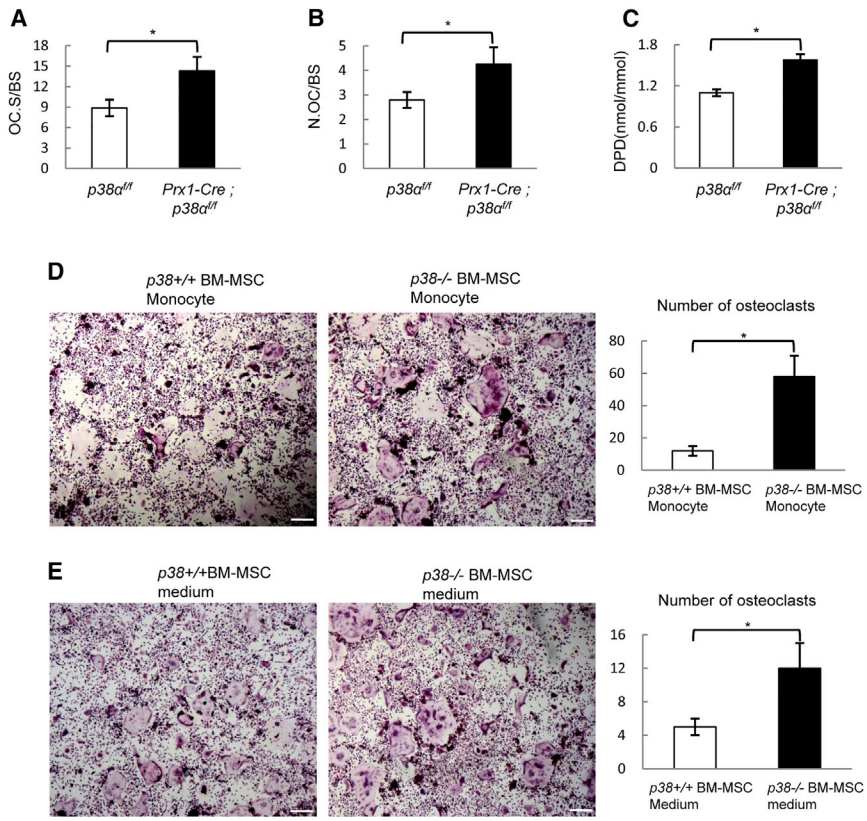

Figure 4. Ablation of *p38α* in *Prx1*+ BM-MSCs Promoted Osteoclastogenesis and Bone Resorption

(A) *Prx1-Cre; p38α$^{f/f}$* mice showed an increase in the osteoclast surface per bone surface. Data represent means ± SEM of eight independent experiments, *p < 0.05.

(B) *Prx1-Cre; p38α$^{f/f}$* mice showed an increase in the number of osteoclasts per bone surface. Data represent means ± SEM of eight independent experiments, *p < 0.05.

(C) *Prx1-Cre; p38α$^{f/f}$* mice showed an increase in the levels of urine DPD. Urine levels of DPD were determined with an ELISA kit and were normalized to urine levels of creatine. Data represent means ± SEM of eight independent experiments, *p < 0.05.

(D) Co-culture experiments showed that *p38α−/−* BM-MSCs had increased potential to support osteoclastogenesis. WT and *p38α−/−* BM-MSCs were plated in BM-MSC culture medium and, after 24 hr, bone marrow monocytes isolated from normal mice were added onto the BM-MSC cultures, which were cultured in the absence of RANKL or M-CSF. After 7 days, the plates were stained for TRAP. Right panel: quantitation data to show the number of osteoclasts per view. Scale bar, 100 μm. Data represent means ± SEM of three independent experiments, *p < 0.05.

(E) *p38α−/−* BM-MSC culture medium also showed increased potential to support osteoclastogenesis. Right panel: quantitation data to show the number of osteoclasts per view. Scale bar, 100 μm. Data represent means ± SEM of three independent experiments, *p < 0.05. See also Figure S4.

p38α knockout mice, nor did it further increase the number of osteoclasts or bone resorption rate (Table 1; Figures 6F and 6G). Note that ovariectomy showed no significant effect on bone formation in WT or *Prx1-Cre; p38α$^{f/f}$* mice, and estradiol did not show any significant effects on the differentiation of BM-MSCs and osteoblasts (Table 1 and data not shown). These results suggest that estrogen deficiency regulates in vivo osteoclastogenesis and bone resorption mainly through p38α-mediated expression of OPG in *Prx1*+ BM-MSCs.

DISCUSSION

As stem cells of the skeleton, BM-MSC's lineage commitment, a crucial step thought to determine the yield of functional osteoblasts, needs to be tightly regulated. Yet how BM-MSC lineage commitment is regulated remains poorly understood. This study revealed that p38α MAPK regulates tri-lineage commitment and proliferation of BM-MSCs. p38α MAPK deficiency compromises osteogenic/chondrogenic differentiation but favors adipogenic differentiation, and results in a decrease in bone mass, a defect in growth plate, and an increase in bone marrow fat. Previous studies have implicated that YAP, C-MAF, and VEGF differentially regulate osteoblast and adipogenic differentiation of BM-MSCs (Hong et al., 2005; Liu et al., 2012; Nishikawa et al., 2010). It will be interesting to test whether there exist links between p38 MAPKs and YAP, C-MAF, or VEGF in the context of BM-MSC lineage commitment. These proteins may present a class of targets for drug development for osteoporosis prevention/treatment.

Our data suggest that p38α may promote BM-MSC osteogenic commitment by suppressing the NF-κB pathway. Previous studies suggest that p38α and p38β promote osteoblast differentiation via modifying RUNX2 and OSX (Greenblatt et al., 2013). But lineage-specific transcription factors such as RUNX2 and OSX are in general not expressed in multipotent BM-MSCs, and thus p38 MAPKs-mediated phosphorylation of these proteins may not be a major factor in determining the cell fates of BM-MSCs (Chang et al., 2009; Yu et al., 2014). Thus, p38α may

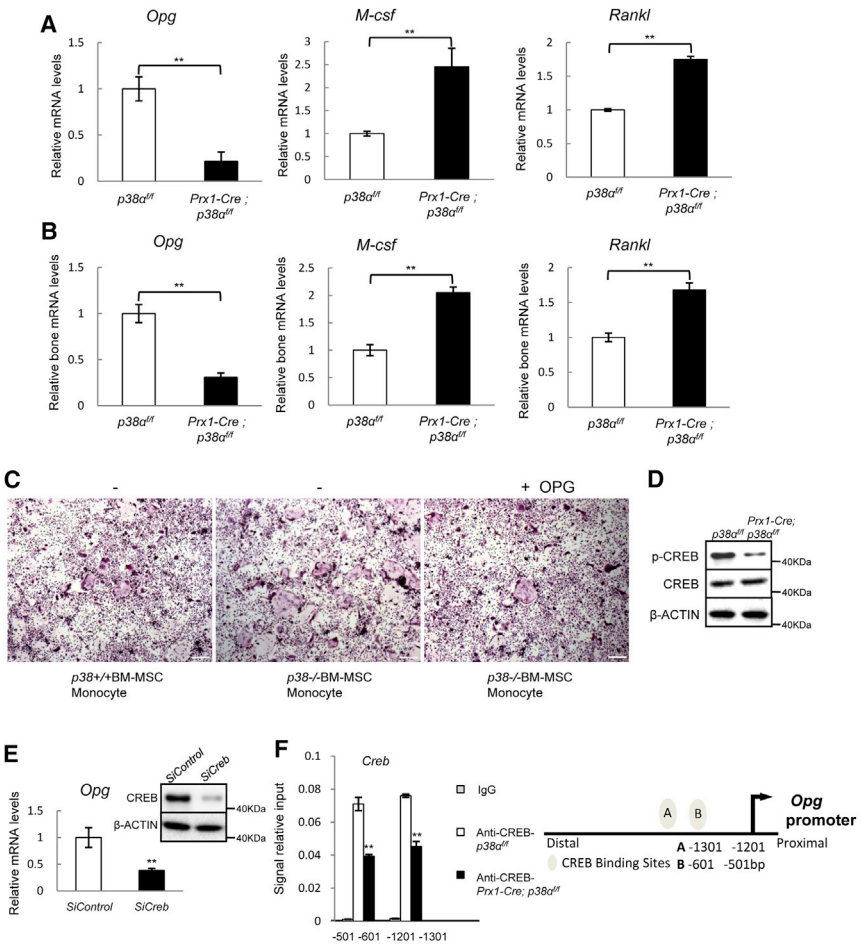

Figure 5. p38α Positively Regulated OPG Expression via CREB

(A) *p38α−/−* BM-MSCs showed a decreased expression of OPG and a modest increase in RANKL and M-CSF compared with WT BM-MSCs. Total RNA was isolated from WT and *p38α−/−* BM-MSCs and was used to determine the mRNA levels of *Opg*, *Rankl*, and *M-csf*. Data represent means ± SEM of three independent experiments, **p < 0.01.

(B) *Prx1-Cre; p38α$^{f/f}$* mouse bones also showed a decrease in *Opg* mRNA levels and a modest increase in *Rankl* and *M-csf*. The femur bones were frozen and total RNA was isolated. Data represent means ± SEM of six independent experiments, **p < 0.01.

(C) Addition of OPG to the *p38α−/−* BM-MSCs co-cultured with normal monocytes impeded the enhanced osteoclast differentiation. The experiments were carried out as described in Figure 4D, except that OPG (20 ng/ml) was added to the cultures. Scale bar, 100 μm.

(D) *p38α−/−* BM-MSCs showed a decrease in CREB phosphorylation. WT and *p38α−/−* BM-MSCs were collected and lysed. The levels of CREB and p-CREB were determined by western blot.

(E) Knockdown of *Creb* led to a down-regulation of *Opg* in normal BM-MSCs. BM-MSCs were transfected with control or siRNA against *Creb*. qPCR was carried out to determine the mRNA levels of *Opg*. Right panel: western blot showing the knockdown of CREB. Data represent means ± SEM of three independent experiments, **p < 0.01.

(F) ChIP experiments showed that *Opg* promoter has two CREB binding sites at −501 to −601 and −1201 to −1301. Right panel: a diagram showing the binding sites of CREB in the promoter of *Opg* gene. Data represent means ± SEM of three independent experiments, **p < 0.01.

regulate BM-MSC osteogenic commitment and osteoblast maturation with different mechanisms (Figure 6H). Moreover, p38α may promote BM-MSC osteogenic commitment by suppressing the competing adipogenic or chondrogenic commitment through down-regulating PPARγ, C/EBPα, and SOX9, transcription factors essential for commitment of these two lineages (Kozhemyakina et al., 2015).

p38α deficiency led to a decrease in the number of osteoblasts on bone sections, which can be caused by defective BM-MSC osteogenic differentiation. Surprisingly, the number of BM-MSCs and the BM-MSC proliferation rate were increased in the absence of p38α. This seeming discrepancy may be explained by the fact that mouse bone marrow may contain MSCs that outnumber the bone multicellular units, where new bone formation is occurring. Although *p38α* ablation leads to overproliferation of BM-MSCs, a large portion of these cells may not be actively involved in bone formation. Thus, the number of BM-MSCs is not directly translated into the number of osteoblasts.

We found that the function of BM-MSC-expressed p38α is not limited to osteoblastogenesis and bone formation. We show that p38α-controlled, CREB-mediated OPG production by BM-MSCs is critical for coupling bone formation and resorption. This is in contrast to the findings that ablation of *p38α* or *p38β* in osteoprogenitors/osteoblasts or *Dermo1*+ cells failed to affect osteoclastogenesis or bone resorption (Greenblatt et al., 2010; Thouverey and Caverzasio, 2012). Thus, only p38α expressed in BM-MSCs but not in osteoblasts is involved in communicating with monocytes/osteoclasts under physiological conditions. One explanation is that in a bone remodeling unit, the newly recruited BM-MSCs may secrete OPG to immediately inhibit further osteoclastogenesis, whereas osteoblast-secreted OPG molecules are embedded in the newly formed bone matrix and are not accessible to monocytes/osteoclasts. Alternatively, osteoblasts may have pathways redundant for p38α-OPG to communicate to osteoclastogenesis under physiological conditions.

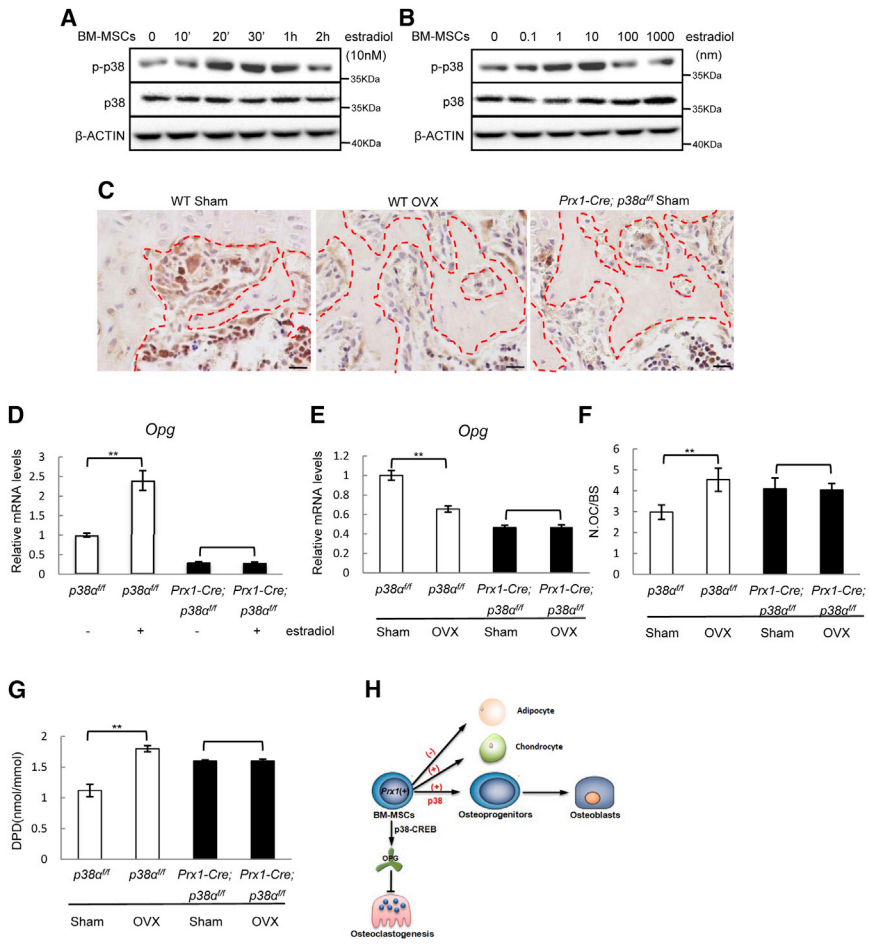

Figure 6. The p38-OPG Axis in BM-MSCs Participated in Estrogen Deficiency-Induced Osteoporosis

(A) Estradiol activated p38 MAPKs in a time-dependent manner in BM-MSCs. Normal BM-MSCs were stimulated with 10 nM of estradiol for different periods of time and the activation of p38 MAPKs was determined by western blot.

(B) Estradiol activated p38 MAPKs in a dose-dependent manner in BM-MSCs.

(C) Ovariectomy diminished p38 MAPKs activation on bone sections. WT mice were ovariectomized or sham-operated. The femur bones were decalcified, and immuno-stained for p-p38 MAPKs. The bone from *Prx1-Cre; p38α$^{f/f}$* mice was used as a negative control. The red dashed lines mark the bone surfaces. Scale bar, 100 μm.

(D) Estradiol induced *Opg* expression in a p38α-dependent manner. WT and *p38α−/−* BM-MSCs were treated with estradiol for 24 hr and the mRNA levels of *Opg* were determined with qPCR. Data represent means ± SEM of three independent experiments, **p < 0.01.

(E) Ovariectomy down-regulated *Opg* expression in the bone in a p38α-dependent manner. Total RNA was isolated from femur bones and *Opg* levels were determined with qPCR. Data represent means ± SEM of three independent experiments, **p < 0.01.

(F) Ovariectomy did not further increase the number of osteoclasts in *Prx1-Cre; p38α$^{f/f}$* mice. Data represent means ± SEM of eight independent experiments, **p < 0.01.

(G) Ovariectomy did not further increase the level of urine DPD levels in *Prx1-Cre; p38α$^{f/f}$* mice. Data represent means ± SEM of eight independent experiments, **p < 0.01.

(H) A diagram showing how p38α is involved in osteoblastogenesis, osteoclastogenesis, and their coordination during bone remodeling. See also Figure S5.

The p38-CREB-OPG pathway in BM-MSCs is also under the control of estrogen. We show that p38α MAPK can be activated by estrogen and that p38α is also required for optimal expression of ERα. Activated p38α mediates estrogen-induced OPG expression in BM-MSCs, which helps to maintain the bone mass under physiological conditions. Estrogen deficiency leads to a decrease in p38α MAPK activation and OPG synthesis, leading to an increase in osteoclastogenesis and bone resorption (Figure 6H). As such, *Prx1*+ BM-MSC-specific deletion of *p38α* renders the mice resistant to estrogen deficiency-induced bone loss. Interestingly, a recent study reported that mice with *p38α* ablated in osteoblasts are also resistant to ovariectomy-induced bone loss, likely via RANKL and interleukin 6 (IL6) (Thouverey and Caverzasio, 2015b). These results confirm the important role for p38α in BM-MSCs and osteoblasts in communicating to osteoclastogenesis under estrogen-deficient conditions, although these two cells may use different mechanisms. While recent studies suggest that estrogen may promote osteoclast apoptosis and thus inhibit bone resorption to preserve the bone (Krum et al., 2008; Nakamura et al., 2007), these findings suggest that the contribution of BM-MSC/osteoblast-osteoclast coupling to the pathogenesis of postmenopausal osteoporosis may be greater than previously thought.

Previous studies have shown that BM-MSCs can be labeled by markers including *Prx1*, *Dermo1*, *leptin receptor*, and *Nestin* (Mendelson and Frenette, 2014; Morrison and Scadden, 2014). Our lineage-tracing experiments confirm that *Prx1*+ BM-MSCs can differentiate into osteoblasts, chondrocytes, and adipocytes in vivo. Moreover, deletion of *p38α MAPK* in *Prx1*+ cells affects bone mass, growth

plates, and bone marrow fat, as well as osteoclastogenesis and bone resorption. However, deletion of *p38α* in *Dermo1*+ cells, like deletion of *p38α* in osteoblasts, only affects BM-MSC osteogenic differentiation and bone formation. These results suggest that *Prx1* may be a much early marker than *Dermo1* and that *Dermo1*+ cells may represent a BM-MSC population with limited chondrogenic activity.

In summary, the present study shows that BM-MSC-expressed p38α may take two routes to maintain bone mass and prevent the development of osteoporosis. In particular, p38α is required for proper BM-MSC osteogenic commitment, via the TAK1-NFκB pathway, to maintain proper bone formation, and for OPG synthesis by BM-MSCs to constrain osteoclastogenesis and bone resorption. Moreover, estrogen appears to go through the p38-OPG pathway to preserve the bone. Cytokines or growth factors that can activate p38 MAPKs, e.g., TGFβ1, BMPs, TNFα, and IL6 (Cuadrado and Nebreda, 2010; Han and Sun, 2007; Sorrentino et al., 2008; Yamashita et al., 2008), may regulate bone remodeling via p38α as well.

EXPERIMENTAL PROCEDURES

Mice and Genotyping

The *p38α*$^{f/f}$ mouse line was generated in Dr. Yibin Wang's laboratory at UCLA. The *Dermo1-Cre*, *Prx1-Cre*, *Rosa-LacZ*, and *Rosa-tdTamato* mouse lines were purchased from The Jackson Laboratories. These mice were housed in a pathogen-free facility at the Bio-X Institutes at Shanghai Jiao Tong University and the experimental protocol was approved by the Animal Welfare Committee of the University.

Bone Histomorphometry

Two-month-old mice were injected twice with calcein at a dose of 0.2 mg/20 g body weight with an interval of 7 days and were sacrificed 1 day after the second injection. Bone histomorphometry analysis was carried out following a protocol that has been previously described (Kua et al., 2012; Ma et al., 2012). Briefly, the femurs were removed and fixed in 4% paraformaldehyde (PFA) overnight and then stored in 70% alcohol for future experiments. The bones were dehydrated in 95% ethanol overnight, 100% ethanol for 5 hr, 100% ethanol again overnight, and then transferred into xylene overnight, and vacuumed for 30 min. The bones were then embedded with resin, sliced, and stained with Villanueva-Goldner's one-step trichrome method. All bone-specific parameters were measured and expressed in units following the guidelines established by the American Society for Bone and Mineral Research histomorphometry nomenclature committee using OsteoMeasure software (OsteoMetrics).

Deoxypyridinoline Measurement

Deoxypyridinoline in the urine was determined to evaluate the bone resorption rate, following the procedure recommended by the manufacturer MicroVue (Quidel).

Bone Marrow Smear and Colony-Forming Unit Assay

Bone marrow cells were flushed out onto slides using α-MEM (Sigma), followed by oil red O and DAPI staining. Adipocytes and total marrow cells were counted on ten randomly selected fields of each smear. Adipocyte number is expressed as a percentage of the total numbers of bone marrow cells. To determine colony-forming units, bone marrow cells were prepared, with red blood cells lysed, and plated at 5×10^6 per well in six-well plates. Fresh complete α-MEM medium was changed every 3 days. Seven days later, the plates were washed with cold PBS, fixed with 4% PFA for 30 min, and stained for ALP (Sigma).

Assays for BM-MSC Osteogenic, Chondrogenic, and Adipogenic Differentiation

Bone marrow MSCs were isolated from control and mutant mice, which were expanded in BM-MSC stem cell medium to prevent differentiation. BM-MSCs at passage 2 were plated and transfected with siRNA for *Tak1* or *NF-κB (p65)*, or control siRNA, induced to differentiate into osteoblasts in the presence of osteogenic differentiation medium, which contains ascorbic acid and β-glycerolphosphate. An Alkaline Phosphatase Kit (Sigma) was used to stain for ALP enzymatic activity, following the manufacture's protocol. To determine mineralization, 21- or 28-day cell cultures were fixed in 4% PFA for 20 min, and stained with alizarin red. Adipogenesis of BM-MSC was induced with a StemPro Adipogenesis Differentiation Kit (Gibco), which was detected by oil red O staining. Chondrogenesis was induced using a StemPro Chondrogenesis Differentiation Kit (Gibco) and staining with 1% Alcian blue solution.

Co-culture of BM-MSC and Monocyte

Co-culture experiments were carried out following a protocol that has been previously described (Kua et al., 2012). Mouse bone marrow was flushed out with α-MEM medium from the femurs and tibias. The monocyte fraction was isolated by centrifugation on a Ficoll plus lymphocyte separation medium gradient (ICN Biomedicals). For co-cultures, primary BM-MSC were plated at 5×10^4 per well in 24-well plates for 24 hr. Upon confluency, freshly isolated bone marrow monocytes were then plated (5×10^5) on top of the BM-MSCs and cultured for 6–10 more days, with the medium being changed every 3 days. The cells were then fixed and stained for tartrate-resistant acidic phosphatase (TRAP) using the Acid Phosphatase, Leukocyte TRAP Kit (Sigma), following the manufacturer's protocol. TRAP-positive multinucleated osteoclasts were counted (≥3 nuclei).

Immunohistochemical Staining and TUNEL Assay

Detection of p-p38MAPK was performed on paraffin sections of femur or tibia by immunohistochemistry staining. Tissue sections were processed with an antigen retrieval step before they were incubated with anti-p-p38 antibodies overnight at 4°C. These slides were then washed three times with PBS, incubated with horseradish peroxidase-labeled anti-rabbit antibody for 30 min at 37°C, and developed with diaminobenzidine tetrahydrochloride and hydrogen peroxide in PBS. Cell proliferation and apoptosis were determined by KI67 immunofluorescence staining (Abcam, ab15580) and TUNEL assay (In Situ Cell Death Detection Kit Fluorescein, Roche), respectively.

Western Blot Analysis

BM-MSC or osteoclasts were lysed with TNEN buffer supplemented with protease inhibitors and phosphatase inhibitors. Protein concentration was determined using a Bio-Rad assay. Twenty micrograms of protein lysates of each sample was subjected to SDS-PAGE analysis and transferred onto nitrocellulose membranes. The proteins were detected with specific antibodies (listed in the Supplemental Information).

ChIP Assays

ChIP assays were carried out following the protocol from the SimpleChIP Enzymatic Chromatin IP Kit (Cell Signaling, 9002). Briefly, BM-MSCs or osteoclasts (4×10^7) were treated with 1% formaldehyde for 10 min at room temperature to crosslink proteins to DNA. The chromatin was harvested and fragmented using enzymatic digestion. An aliquot of each sample was set aside as input control, while the remaining portion was subjected to immunoprecipitation with anti-CREB antibodies (Upstate, 05767) overnight at 4°C, with IgG (Beyotime) as control. Immunoprecipitated complex was treated with protease and the DNA was amplified by PCR using primer pairs designed to amplify about 100-bp fragments spanning the 2-kb *Opg* promoter (BM-MSCs).

Data Analysis

For bone histomorphometry analysis, eight mutant and eight control mice were used. For ex vivo studies, at least three pairs of mice were used. In vitro experiments were repeated three times. Results are presented as means ± SEM. Statistical comparisons were performed using unpaired Student's two-tailed t test. $p < 0.05$ was considered statistically significant ($^*p < 0.05$, $^{**}p < 0.01$ when mutant mice were compared with control mice, siRNA knockdown cells were compared with control cells, or the inhibitor-treated group were compared with control group).

SUPPLEMENTAL INFORMATION

Supplemental Information includes Supplemental Experimental Procedures, five figures, and one table and can be found with this article online at http://dx.doi.org/10.1016/j.stemcr.2016.02.001.

AUTHOR CONTRIBUTIONS

Q.C., H.J., S.B., P.L., S.Q., Q.D., G.M., and J.F.L.C. performed the experiments. Y.W. and X.G. contributed to the animal work. Q.C., Z.L.Z., X.J., H.L., B.L. planned the experiments, analyzed the data, and wrote the manuscript.

ACKNOWLEDGMENTS

We would like to thank Lina Gao for technical assistance. The work is supported by the National Key Scientific Program (2012CB966901 and 2014CB942902), National Natural Science Foundation of China (81130039, 31300684, and 81121001), and Shanghai Zhangjiang Stem Cell Research Project (ZJ2014-ZD-002).

Received: September 7, 2015
Revised: February 1, 2016
Accepted: February 1, 2016
Published: March 3, 2016

REFERENCES

Baldridge, D., Shchelochkov, O., Kelley, B., and Lee, B. (2010). Signaling pathways in human skeletal dysplasias. Annu. Rev. Genomics Hum. Genet. *11*, 189–217.

Berendsen, A.D., and Olsen, B.R. (2014). Osteoblast-adipocyte lineage plasticity in tissue development, maintenance and pathology. Cell Mol. Life Sci. *71*, 493–497.

Chang, J., Wang, Z., Tang, E., Fan, Z., McCauley, L., Franceschi, R., Guan, K., Krebsbach, P.H., and Wang, C.Y. (2009). Inhibition of osteoblastic bone formation by nuclear factor-kappaB. Nat. Med. *15*, 682–689.

Cheung, P.C., Campbell, D.G., Nebreda, A.R., and Cohen, P. (2003). Feedback control of the protein kinase TAK1 by SAPK2a/p38alpha. EMBO J. *22*, 5793–5805.

Crane, J.L., and Cao, X. (2014). Bone marrow mesenchymal stem cells and TGF-beta signaling in bone remodeling. J. Clin. Invest. *124*, 466–472.

Cuadrado, A., and Nebreda, A.R. (2010). Mechanisms and functions of p38 MAPK signalling. Biochem. J. *429*, 403–417.

Edwards, J.R., and Mundy, G.R. (2011). Advances in osteoclast biology: old findings and new insights from mouse models. Nat. Rev. Rheumatol. *7*, 235–243.

Engin, F., and Lee, B. (2010). NOTCHing the bone: insights into multi-functionality. Bone *46*, 274–280.

Greenbaum, A., Hsu, Y.M., Day, R.B., Schuettpelz, L.G., Christopher, M.J., Borgerding, J.N., Nagasawa, T., and Link, D.C. (2013). CXCL12 in early mesenchymal progenitors is required for haematopoietic stem-cell maintenance. Nature *495*, 227–230.

Greenblatt, M.B., Shim, J.H., Zou, W., Sitara, D., Schweitzer, M., Hu, D., Lotinun, S., Sano, Y., Baron, R., Park, J.M., et al. (2010). The p38 MAPK pathway is essential for skeletogenesis and bone homeostasis in mice. J. Clin. Invest. *120*, 2457–2473.

Greenblatt, M.B., Shim, J.H., and Glimcher, L.H. (2013). Mitogen-activated protein kinase pathways in osteoblasts. Annu. Rev. Cell Dev. Biol. *29*, 63–79.

Guihard, P., Danger, Y., Brounais, B., David, E., Brion, R., Delecrin, J., Richards, C.D., Chevalier, S., Redini, F., Heymann, D., et al. (2012). Induction of osteogenesis in mesenchymal stem cells by activated monocytes/macrophages depends on oncostatin M signaling. Stem Cells *30*, 762–772.

Han, J., and Sun, P. (2007). The pathways to tumor suppression via route p38. Trends Biochem. Sci. *32*, 364–371.

Harada, S., and Rodan, G.A. (2003). Control of osteoblast function and regulation of bone mass. Nature *423*, 349–355.

Henriksen, K., Karsdal, M.A., and Martin, T.J. (2014). Osteoclast-derived coupling factors in bone remodeling. Calcif. Tissue Int. *94*, 88–97.

Hofbauer, L.C., Khosla, S., Dunstan, C.R., Lacey, D.L., Spelsberg, T.C., and Riggs, B.L. (1999). Estrogen stimulates gene expression and protein production of osteoprotegerin in human osteoblastic cells. Endocrinology *140*, 4367–4370.

Hong, J.H., Hwang, E.S., McManus, M.T., Amsterdam, A., Tian, Y., Kalmukova, R., Mueller, E., Benjamin, T., Spiegelman, B.M., Sharp,

P.A., et al. (2005). TAZ, a transcriptional modulator of mesenchymal stem cell differentiation. Science *309*, 1074–1078.

Hu, Y.Y., Chan, E., Wang, S.X., and Li, B.J. (2003). Activation of p38 mitogen-activated protein kinase is required for osteoblast differentiation. Endocrinology *144*, 2068–2074.

Hutchison, M.R. (2013). Mice with a conditional deletion of the neurotrophin receptor TrkB are dwarfed, and are similar to mice with a MAPK14 deletion. PLoS One *8*, e66206.

Karsenty, G. (2008). Transcriptional control of skeletogenesis. Annu. Rev. Genomics Hum. Genet. *9*, 183–196.

Kassem, M., and Marie, P.J. (2011). Senescence-associated intrinsic mechanisms of osteoblast dysfunctions. Aging Cell *10*, 191–197.

Kearns, A.E., Khosla, S., and Kostenuik, P.J. (2008). Receptor activator of nuclear factor kappaB ligand and osteoprotegerin regulation of bone remodeling in health and disease. Endocr. Rev. *29*, 155–192.

Kozhemyakina, E., Lassar, A.B., and Zelzer, E. (2015). A pathway to bone: signaling molecules and transcription factors involved in chondrocyte development and maturation. Development *142*, 817–831.

Krum, S.A., Miranda-Carboni, G.A., Hauschka, P.V., Carroll, J.S., Lane, T.F., Freedman, L.P., and Brown, M. (2008). Estrogen protects bone by inducing Fas ligand in osteoblasts to regulate osteoclast survival. EMBO J. *27*, 535–545.

Kua, H.Y., Liu, H., Leong, W.F., Li, L., Jia, D., Ma, G., Hu, Y., Wang, X., Chau, J.F., Chen, Y.G., et al. (2012). c-Abl promotes osteoblast expansion by differentially regulating canonical and non-canonical BMP pathways and p16INK4a expression. Nat. Cell Biol. *14*, 727–737.

Lacey, D.L., Boyle, W.J., Simonet, W.S., Kostenuik, P.J., Dougall, W.C., Sullivan, J.K., San Martin, J., and Dansey, R. (2012). Bench to bedside: elucidation of the OPG-RANK-RANKL pathway and the development of denosumab. Nat. Rev. Drug Discov. *11*, 401–419.

Lecka-Czernik, B., and Stechschulte, L.A. (2014). Bone and fat: a relationship of different shades. Arch. Biochem. Biophys. *561*, 124–129.

Lian, J.B., Stein, G.S., van Wijnen, A.J., Stein, J.L., Hassan, M.Q., Gaur, T., and Zhang, Y. (2011). MicroRNA control of bone formation and homeostasis. Nat. Rev. Endocrinol. *8*, 212–227.

Liu, Y.Q., Berendsen, A.D., Jia, S.D., Lotinun, S., Baron, R., Ferrara, N., and Olsen, B.R. (2012). Intracellular VEGF regulates the balance between osteoblast and adipocyte differentiation. J. Clin. Invest. *122*, 3101–3113.

Logan, M., Martin, J.F., Nagy, A., Lobe, C., Olson, E.N., and Tabin, C.J. (2002). Expression of Cre Recombinase in the developing mouse limb bud driven by a Prxl enhancer. Genesis *33*, 77–80.

Long, F. (2012). Building strong bones: molecular regulation of the osteoblast lineage. Nat. Rev. Mol. Cell Biol. *13*, 27–38.

Ma, G., Li, L., Hu, Y., Chau, J.F., Au, B.J., Jia, D., Liu, H., Yeh, J., He, L., Hao, A., et al. (2012). Atypical Atm-p53 genetic interaction in osteogenesis is mediated by Smad1 signaling. J. Mol. Cell Biol. *4*, 118–120.

Manolagas, S.C., O'Brien, C.A., and Almeida, M. (2013). The role of estrogen and androgen receptors in bone health and disease. Nat. Rev. *9*, 699–712.

Mendelson, A., and Frenette, P.S. (2014). Hematopoietic stem cell niche maintenance during homeostasis and regeneration. Nat. Med. *20*, 833–846.

Michael, H., Harkonen, P.L., Vaananen, H.K., and Hentunen, T.A. (2005). Estrogen and testosterone use different cellular pathways to inhibit osteoclastogenesis and bone resorption. J. Bone Miner. Res. *20*, 2224–2232.

Morrison, S.J., and Scadden, D.T. (2014). The bone marrow niche for haematopoietic stem cells. Nature *505*, 327–334.

Nakamura, T., Imai, Y., Matsumoto, T., Sato, S., Takeuchi, K., Igarashi, K., Harada, Y., Azuma, Y., Krust, A., Yamamoto, Y., et al. (2007). Estrogen prevents bone loss via estrogen receptor alpha and induction of Fas ligand in osteoclasts. Cell *130*, 811–823.

Nishikawa, K., Nakashima, T., Takeda, S., Isogai, M., Hamada, M., Kimura, A., Kodama, T., Yamaguchi, A., Owen, M.J., Takahashi, S., et al. (2010). Maf promotes osteoblast differentiation in mice by mediating the age-related switch in mesenchymal cell differentiation. J. Clin. Invest. *120*, 3455–3465.

Oh, C.D., Chang, S.H., Yoon, Y.M., Lee, S.J., Lee, Y.S., Kang, S.S., and Chun, J.S. (2000). Opposing role of mitogen-activated protein kinase subtypes, erk-1/2 and p38, in the regulation of chondrogenesis of mesenchymes. J. Bio Chem. *275*, 5613–5619.

Ortuno, M.J., Susperregui, A.R., Artigas, N., Rosa, J.L., and Ventura, F. (2013). Osterix induces Col1a1 gene expression through binding to Sp1 sites in the bone enhancer and proximal promoter regions. Bone *52*, 548–556.

Pederson, L., Ruan, M., Westendorf, J.J., Khosla, S., and Oursler, M.J. (2008). Regulation of bone formation by osteoclasts involves Wnt/BMP signaling and the chemokine sphingosine-1-phosphate. Proc. Natl. Acad. Sci. USA *105*, 20764–20769.

Phimphilai, M., Zhao, Z., Boules, H., Roca, H., and Franceschi, R.T. (2006). BMP signaling is required for RUNX2-dependent induction of the osteoblast phenotype. J. Bone Miner. Res. *21*, 637–646.

Qin, X., Jiang, Q., Matsuo, Y., Kawane, T., Komori, H., Moriishi, T., Taniuchi, I., Ito, K., Kawai, Y., Rokutanda, S., et al. (2015). Cbfb regulates bone development by stabilizing runx family proteins. J. Bone Miner. Res. *30*, 706–714.

Rachner, T.D., Khosla, S., and Hofbauer, L.C. (2011). Osteoporosis: now and the future. Lancet *377*, 1276–1287.

Rodriguez-Carballo, E., Gamez, B., Sedo-Cabezon, L., Sanchez-Feutrie, M., Zorzano, A., Manzanares-Cespedes, C., Rosa, J.L., and Ventura, F. (2014). The p38 alpha MAPK function in osteoprecursors is required for bone formation and bone homeostasis in adult mice. PLoS One *9*, e102032.

Sorrentino, A., Thakur, N., Grimsby, S., Marcusson, A., von Bulow, V., Schuster, N., Zhang, S., Heldin, C.H., and Landstrom, M. (2008). The type I TGF-beta receptor engages TRAF6 to activate TAK1 in a receptor kinase-independent manner. Nat. Cell Biol. *10*, 1199–1207.

Stanton, L.A., Sabari, S., Sampaio, A.V., Underhill, T.M., and Beier, F. (2004). p38 MAP kinase signalling is required for hypertrophic chondrocyte differentiation. Biochem. J. *378*, 53–62.

Takeshita, S., Fumoto, T., Matsuoka, K., Park, K.A., Aburatani, H., Kato, S., Ito, M., and Ikeda, K. (2013). Osteoclast-secreted CTHRC1 in the coupling of bone resorption to formation. J. Clin. Invest. *123*, 3914–3924.

Thouverey, C., and Caverzasio, J. (2012). The p38alpha MAPK positively regulates osteoblast function and postnatal bone acquisition. Cell Mol. Life Sci. *69*, 3115–3125.

Thouverey, C., and Caverzasio, J. (2015a). Focus on the p38 MAPK signaling pathway in bone development and maintenance. Bonekey Rep. *4*, 711.

Thouverey, C., and Caverzasio, J. (2015b). Ablation of p38α MAPK signaling in osteoblast lineage cells protects mice from bone loss induced by estrogen deficiency. Endocrinology *156*, 4377–4387.

Tran, T.H., Jarrell, A., Zentner, G.E., Welsh, A., Brownell, I., Scacheri, P.C., and Atit, R. (2010). Role of canonical Wnt signaling/beta-catenin via Dermo1 in cranial dermal cell development. Development *137*, 3973–3984.

Wagner, E.F., and Nebreda, A.R. (2009). Signal integration by JNK and p38 MAPK pathways in cancer development. Nat. Rev. Cancer *9*, 537–549.

Wang, X.Y., Goh, C.H., and Li, B.J. (2007). p38 Mitogen-activated protein kinase regulates osteoblast differentiation through Osterix. Endocrinology *148*, 1629–1637.

Wu, J.Y., Scadden, D.T., and Kronenberg, H.M. (2009). Role of the osteoblast lineage in the bone marrow hematopoietic niches. J. Bone Miner. Res. *24*, 759–764.

Yamashita, M., Fatyol, K., Jin, C., Wang, X., Liu, Z., and Zhang, Y.E. (2008). TRAF6 mediates Smad-independent activation of JNK and p38 by TGF-beta. Mol. Cell *31*, 918–924.

Yao, Z., Li, Y., Yin, X., Dong, Y., Xing, L., and Boyce, B.F. (2014). NF-kappaB RelB negatively regulates osteoblast differentiation and bone formation. J. Bone Miner. Res. *29*, 866–877.

Yu, K., Xu, J., Liu, Z., Sosic, D., Shao, J., Olson, E.N., Towler, D.A., and Ornitz, D.M. (2003). Conditional inactivation of FGF receptor 2 reveals an essential role for FGF signaling in the regulation of osteoblast function and bone growth. Development *130*, 3063–3074.

Yu, B., Chang, J., Liu, Y., Li, J., Kevork, K., Al-Hezaimi, K., Graves, D.T., Park, N.H., and Wang, C.Y. (2014). Wnt4 signaling prevents skeletal aging and inflammation by inhibiting nuclear factor-kappaB. Nat. Med. *20*, 1009–1017.

Zaidi, M., Buettner, C., Sun, L., and Iqbal, J. (2012). Minireview: the link between fat and bone: does mass beget mass? Endocrinology *153*, 2070–2075.

Zhang, R., Murakami, S., Coustry, F., Wang, Y., and de Crombrugghe, B. (2006). Constitutive activation of MKK6 in chondrocytes of transgenic mice inhibits proliferation and delays endochondral bone formation. Proc. Natl. Acad. Sci. USA *103*, 365–370.

Stem Cell Reports, Volume *6*

Supplemental Information

p38α MAPK Regulates Lineage Commitment and OPG Synthesis of Bone Marrow Stromal Cells to Prevent Bone Loss under Physiological and Pathological Conditions

Qian Cong, Hao Jia, Soma Biswas, Ping Li, Shoutao Qiu, Qi Deng, Xizhi Guo, Gang Ma, Jenny Fang Ling Chau, Yibin Wang, Zhen-Lin Zhang, Xinquan Jiang, Huijuan Liu, and Baojie Li

Figure S1

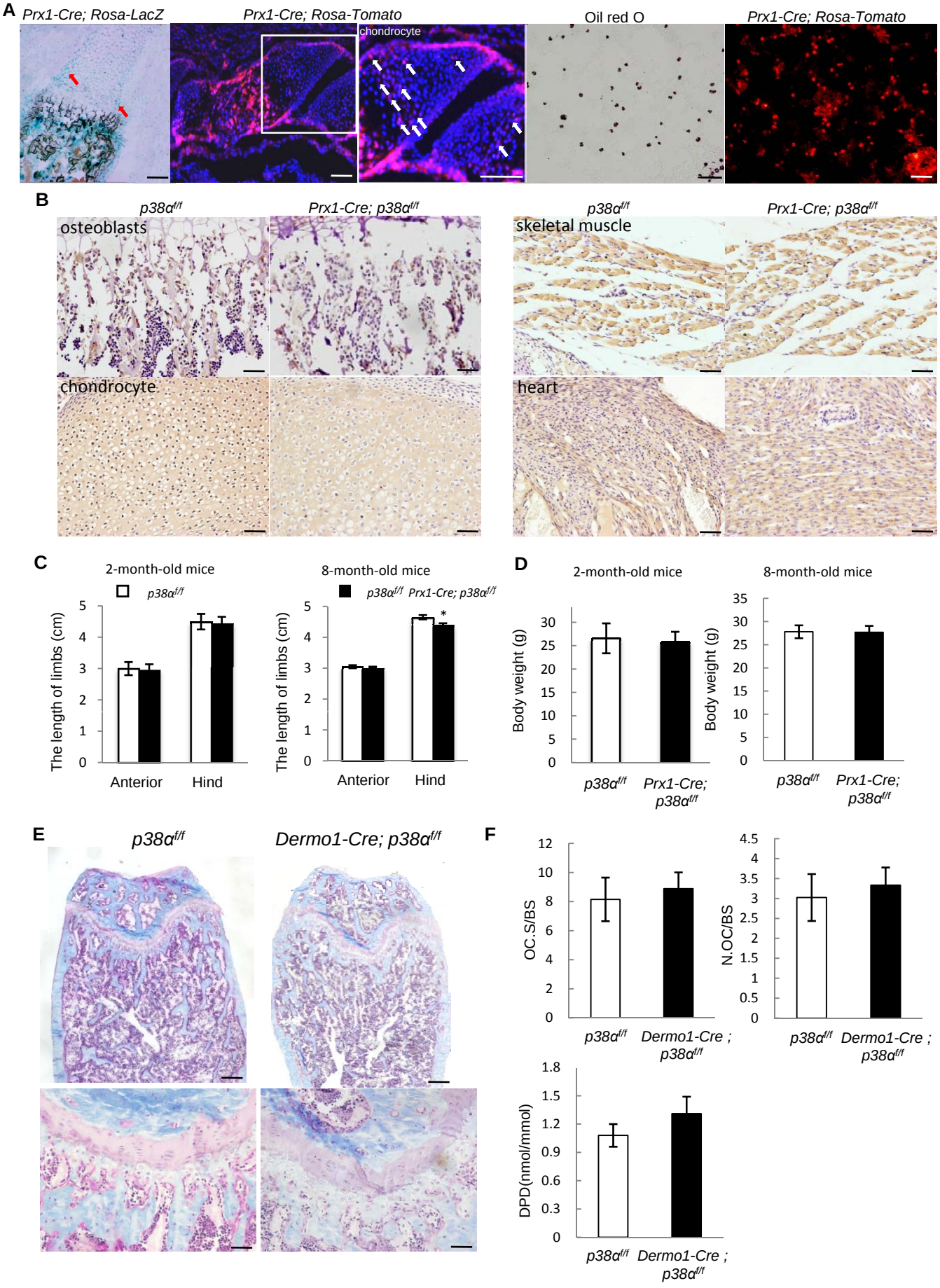
A
Prx1-Cre; Rosa-LacZ
Prx1-Cre; Rosa-Tomato
chondrocyte
Oil red O
Prx1-Cre; Rosa-Tomato
B
p38α f/f
Prx1-Cre; p38α f/f
osteoblasts
chondrocyte
skeletal muscle
heart
C
2-month-old mice
8-month-old mice
p38α f/f
Prx1-Cre; p38α f/f
The length of limbs (cm)
Anterior
Hind
D
2-month-old mice
8-month-old mice
Body weight (g)
p38α f/f
Prx1-Cre; p38α f/f
E
p38α f/f
Dermo1-Cre; p38α f/f
F
OC.S/BS
N.OC/BS
DPD(nmol/mmol)
p38α f/f
Dermo1-Cre ; p38α f/f

Figure S2

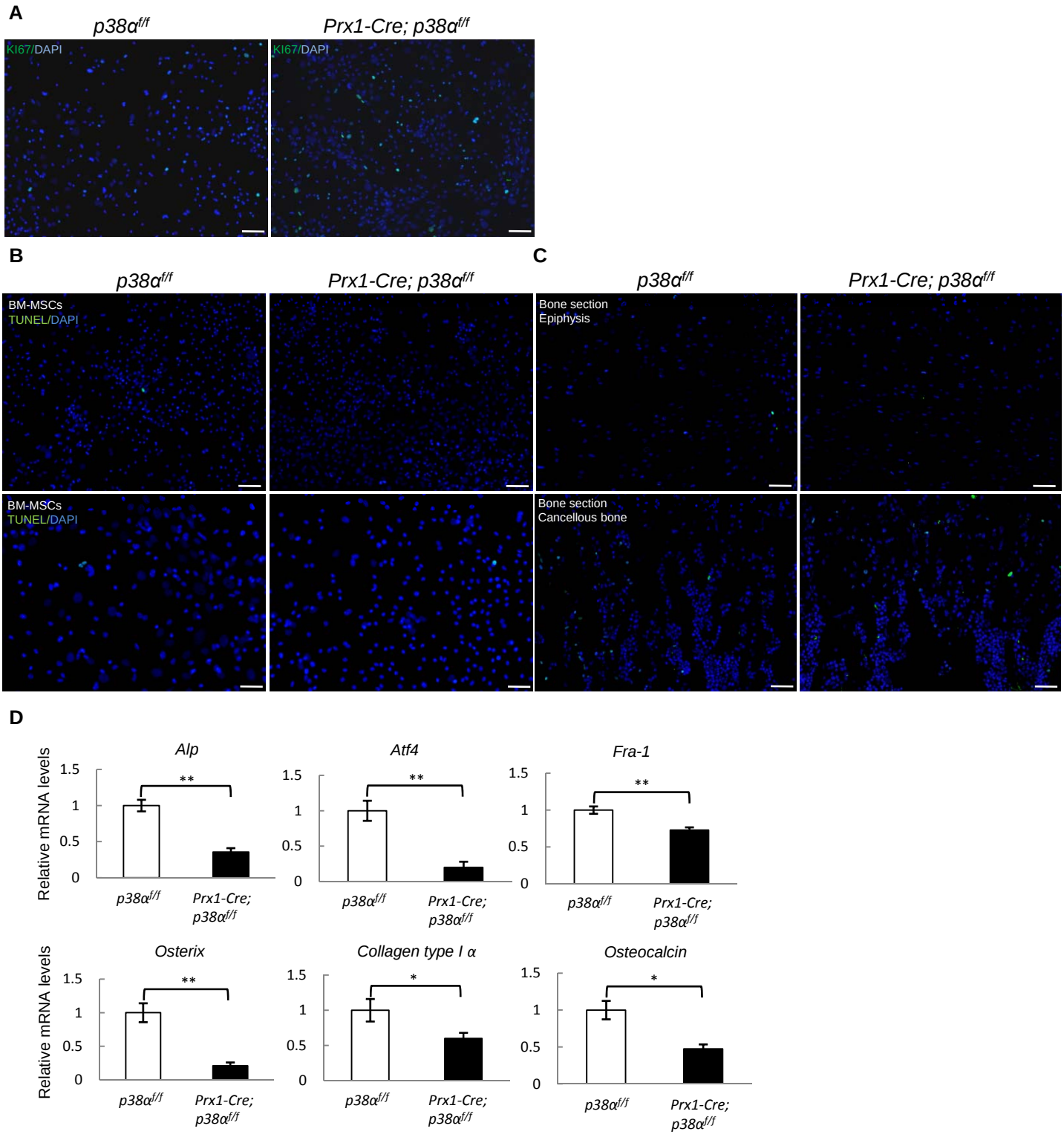
A
p38α f/f
Prx1-Cre; p38α f/f
KI67/DAPI
KI67/DAPI
B
p38α f/f
Prx1-Cre; p38α f/f
BM-MSCs
TUNEL/DAPI
BM-MSCs
TUNEL/DAPI
C
p38α f/f
Prx1-Cre; p38α f/f
Bone section
Epiphysis
Bone section
Cancellous bone
D
Alp
Atf4
Fra-1
Osterix
Collagen type I α
Osteocalcin
Relative mRNA levels
1.5
1
0.5
0
**
*
p38α f/f
Prx1-Cre; p38α f/f

Figure S3

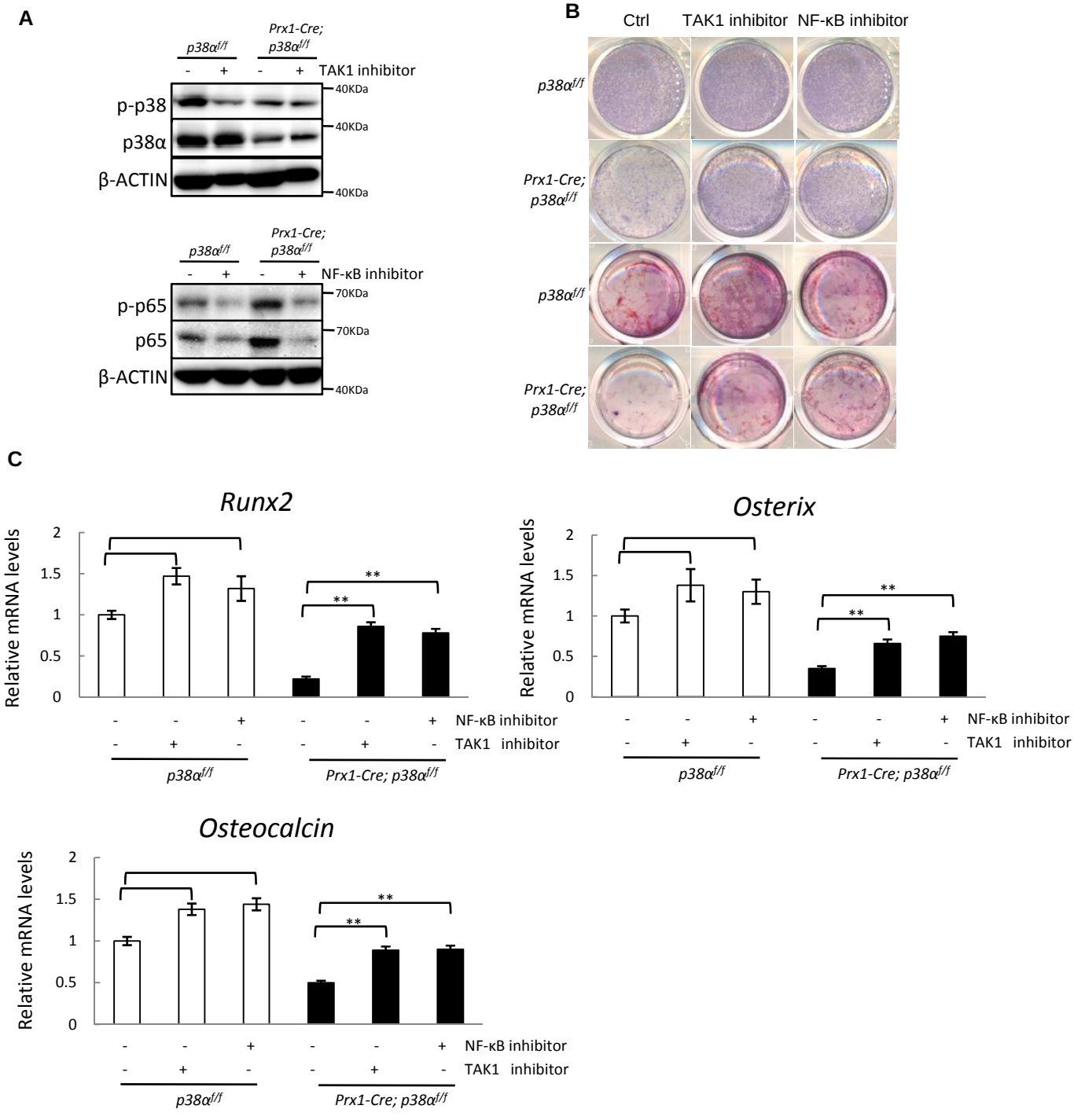
A
p38α f/f
Prx1-Cre; p38α f/f
- + - +
TAK1 inhibitor
p-p38
p38α
β-ACTIN
40KDa
40KDa
40KDa
NF-κB inhibitor
p-p65
p65
β-ACTIN
70KDa
70KDa
40KDa
B
Ctrl
TAK1 inhibitor
NF-κB inhibitor
p38α f/f
Prx1-Cre; p38α f/f
p38α f/f
Prx1-Cre; p38α f/f
C
Runx2
Osterix
Osteocalcin
Relative mRNA levels
0
0.5
1
1.5
2
**
**
- - + - - + NF-κB inhibitor
- + - - + - TAK1 inhibitor
p38α f/f
Prx1-Cre; p38α f/f

Figure S4

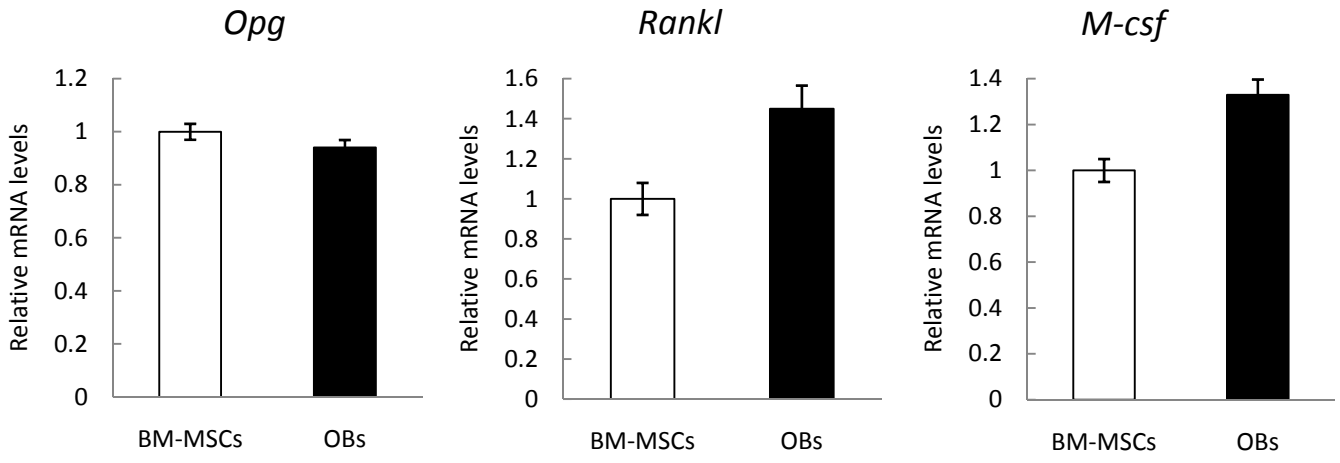
Opg
Relative mRNA levels
1.2
1
0.8
0.6
0.4
0.2
0
BM-MSCs
OBs
Rankl
Relative mRNA levels
1.6
1.4
1.2
1
0.8
0.6
0.4
0.2
0
BM-MSCs
OBs
M-csf
Relative mRNA levels
1.4
1.2
1
0.8
0.6
0.4
0.2
0
BM-MSCs
OBs

Figure S5

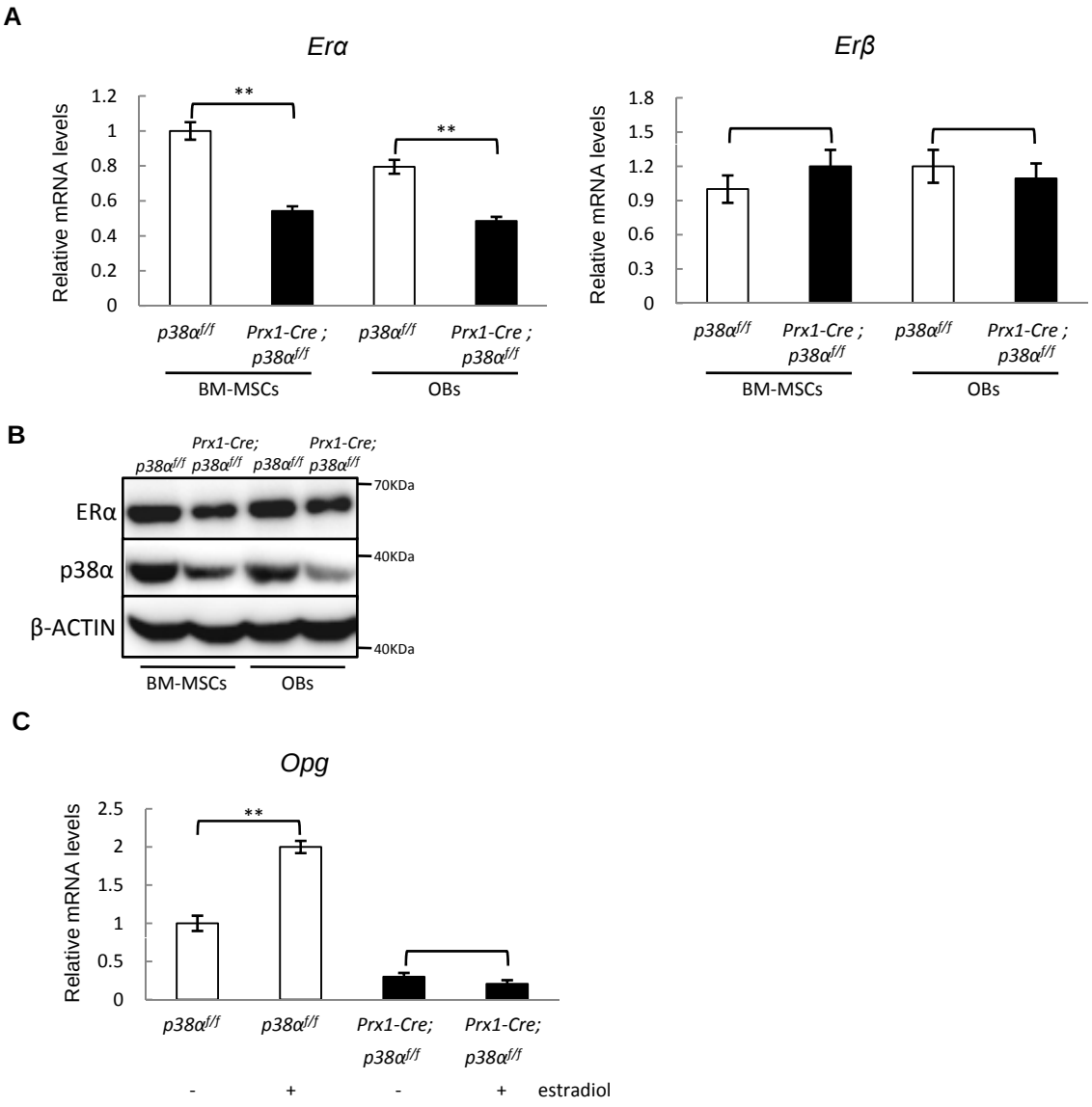
A
Erα
Erβ
Relative mRNA levels
**
**
p38α f/f
Prx1-Cre ; p38α f/f
BM-MSCs
OBs
B
Prx1-Cre; p38α f/f
ERα
p38α
β-ACTIN
70KDa
40KDa
40KDa
BM-MSCs
OBs
C
Opg
Relative mRNA levels
**
p38α f/f
Prx1-Cre; p38α f/f
estradiol

Supplemental Figure Legends

Figure S1. Ablation of *p38α* in *Prx1*+ BM-MSCs leads to shortened limb length, related to Figure 1. (A) Lineage tracing of *Prx1*+ cell in the osteoblasts, chondrocytes, and bone marrow fat in mouse. New-born *Prx1-Cre; Rosa-tdTomato* and *Rosa-LacZ* mice were used (Scale bar, 100 μm). The bone marrow smear was used to detect bone marrow adipocytes in adult *Prx1-Cre; Rosa-tdTomato* (Scale bar, 50 μm). Arrows indicate chondrocytes. (B) Immunohistochemical staining shows that p-p38 was greatly reduced in the bone but not in the heart or skeletal muscle of *Prx1-Cre; p38α$^{f/f}$* mice. Scale bar, 50 μm. (C) The hind limb was slightly shortened in 8-month-old *Prx1-Cre; p38α$^{f/f}$* mice. (D) Two or eight-month-old *Prx1-Cre; p38α$^{f/f}$* mice showed normal body weight. Data represent means ± SEM of eight independent experiments, *$p<0.05$ when the value in mutant mice was compared to that of control mice. (E) *Dermo1-Cre; p38α$^{f/f}$* mice did not show a significant defect in growth plate. Upper panel: Scale bar, 200 μm. Bottom panel: Scale bar, 50 μm. (F) *Dermo1-Cre; p38α$^{f/f}$* mice did not show a significant defect in bone resorption rate. Data represent means ± SEM of eight independent experiments.

Figure S2. BM-MSCs isolated from *Prx1-Cre; p38α$^{f/f}$* mice showed enhanced proliferation and defective osteogenic differentiation without affecting apoptosis, related to Figure 2. (A) *p38α-/-* BM-MSC cultures showed an increase in the number of KI67 positive cells. Scale bar, 100 μm. (B) *p38α-/-* BM-MSC cultures showed no alteration in TUNEL positive cells compared to WT BM-MSC cultures. (C) *Prx1-Cre; p38α$^{f/f}$* mouse femur sections showed no alteration in TUNEL positive cells compared to WT mouse. Scale bar, 100 μm. (D) Quantitative PCR results revealed that *p38α-/-* BM-MSC cultures showed a decrease in the mRNA levels of osteogenic differentiation markers. Data represent means ± SEM of three independent experiments, *$p<0.05$, **$p<0.01$.

Figure S3. Inhibition of TAK1 or NF-κB with small molecule compounds rescued the osteogenic differentiation defect of *p38α-/-* BM-MSCs, related to Figure 3. WT and

p38α-/- BM-MSCs were cultured in osteoblast differentiation medium for 4 days in the presence of TAK1 inhibitor (5Z-7-Oxozeaenol, 0.1 μM) or NF-κB inhibitor (BAY11-7082, 10μM). (A) Western blot results show that inhibition of TAK1 led to a decrease in p38 MAPK activation (upper panel) and inhibition of NF-κB led to a decrease in p65 phosphorylation (bottom panel). (B) The ALP staining results showed that inhibition of TAK1 or NF-κB with small molecule compounds rescued the osteogenic differentiation defect of *p38α-/-* BM-MSCs. (C) Quantitative PCR results confirmed that inhibition of TAK1 or NF-κB with small molecule compounds rescued the osteogenic differentiation defect of *p38α-/-* BM-MSCs. Data represent means ± SEM of three independent experiments, **p<0.01.

Figure S4. BM-MSCs and osteoblasts did not show a significant difference in expression of *Opg*, *Rankl*, or *M-csf*, related to Figure 4. BM-MSCs and differentiated osteoblasts (induced by BMP2) cultures were collected, from which total RAN was isolated. Quantitative PCR was used to determine the mRNA levels of *Opg*, *Rankl*, and *M-csf*, with *Actin* as an internal control. Data represent means ± SEM of three independent experiments.

Figure S5. *p38α-/-* BM-MSCs and osteoblasts showed decreased expression of ERα but not ERβ, related to Figure 6. (A) BM-MSCs and osteoblasts cultures were collected, from which total RNA was isolated. Quantitative PCR was used to determine the mRNA levels of *Erα* and *Erβ*. (B) Western blot showed that *p38α-/-* BM-MSCs and osteoblasts expressed decreased levels of ERα at the protein levels compared to control counterparts. (C) *p38α-/-* osteoblasts also showed a decrease in *Opg* expression in response to estradiol. Data represent means ± SEM of three independent experiments, **p<0.01.

Supplemental Table S1. Histomorphometry parameters of 3-month-old *Dermo1-Cre; p38α$^{f/f}$* and control mice, related to Table 1. Data represent means ± SEM of eight independent experiments, * p<0.05 when the value of mutant mice was compared to that of control mice.

	p38α$^{f/f}$	***Dermo1-Cre; p38α$^{f/f}$***
BV/TV(%)	15.377±1.97	11.11±3.44*
Tb.Ar(%)	13.034±1.45	9.887±2.61*
Tb.Th(mcm)	25.449±2.02	20.333±3.13*
Tb.Sp(mcm)	238.154±20.86	377.625±116.59*
Tb.N(#/mm)	4.655±1.11	3.289±0.99*
MAR(mcm/d)	1.521±0.142	1.339±0.076*
BFR(mcm/d)	70.445±4.125	60.356±3.865*
OB.S/BS(%)	15.489±0.706	13.011±1.42*

Supplemental experimental procedures

Mouse genotyping

Genomic DNA was extracted from mouse tails and used for genotyping by PCR using the following sets of primers. *p38α*$^{f/f}$ -F: 5'-TCCTACGAGCGTCGGCAAGGTG-3'; *p38α*$^{f/f}$ -R: 5'-AGTCCCCGAGAGTTCCTGCCTC-3'; *Cre*-F: 5'-TTTCCCGCAGAACCTGAAGA-3'; *Cre*-R: 5'-GGTGCTAACCAGCGTTTTCGT-3'. *Rosa-LacZ*: *Rosa26WT*-F: 5'-GGAGCGGGAGAAATGGATATG-3'; *Rosa26WT*-R: 5'-AAAGTCGCTCTGTGTTAT-3'; *Rosa26*-F: 5'-AAGCACGTTTCCGACTTGAGTTG-3'; *Rosa26*-R: 5'-CATCAAGGAAACCCTGGACTACTG-3'; *Rosa-tdTamato*: oIMR9020: 5'-AAGGGAGCTGCAGTGGAGTA-3'; oIMR9021: 5'-CCGAAAATCTGTGGGAAGTC-3'; oIMR9103: 5'-GGCATTAAAGCAGCGTATCC-3'; oIMR9105: 5'-CTGTTCCTGTACGGCATGG-3'.

Cell Transfection

Cells were plated and transfected with *Creb* siRNA (sc-35111), *Tak1* siRNA (sc-36607), *Nf-κb p65* siRNA (sc-29411), or control siRNA (sc-37007) using Lipofectamine 2000 (Invitrogen). These cells were harvested after 72-96 hours and total RNA and protein were isolated.

Quantitative PCR

Total RNA was isolated from the cells or femurs with Trizol reagent (Invitrogen). Reverse transcription was performed using Transcriptor First strand cDNA synthesis kit (Roche) with random anchored-oligo (dT) 18 primers. Real-time PCRs were performed using FS Universal SYBR Green Master Premix (Roche). Quantification was normalized to the amounts of endogenous *Gapdh*. The primers used for real-time PCR were:

Osteocalcin F: 5'-AGCAGGAGGGCAATAAGGTAGT-3'

R: 5'-ACCGTAGATGCGTTTGTAGGC-3'.

Runx2 F: 5'-TTTAGGGCGCATTCCTCATC-3'

R: 5'-TGTCCTTGTGGATTAAAAGGACTTG-3'

Osterix F: 5'-ACTCATCCCTATGGCTCGTG-3'

R: 5’-GGTAGGGAGCTGGGTTAAGG-3’

C/ebpα F: 5’-TGGACAAGAACAGCAACGAG-3’

R: 5’-AATCTCCTAGTCCTGGCTTG-3’

Pparγ F: 5’-ACTGCCTATGAGCTCTTCAC-3’

R: 5’-CAATCGGATGGTTCTTCGGA-3’

Collagen type Iα F: 5’-CAAGGTCCTTCTGGATCAAGTG-3’

R: 5’-CCTTTATGCCTCTGTCACCTTG-3’

Atf4 F: 5’-TTCCACTCCAGAGCATTCCT-3’

R: 5’-CAGGTGGGTCATAAGGTTTG-3’

Alp F: 5’-TGAGCGACACGGACAAGA-3’

R: 5’-GGCCTGGTAGTTGTTGTGAG-3’

Sox9 F: 5’-AGTCCCAGCGAACGCACATCA-3’

R: 5’-GTCGTATTGCGAGCGGGTGAT-3’

Opg F: 5’-CACCCTGTGTGAAGAGGCCT-3’

R: 5’-GCAGGCTCTCCATCAAGGCA-3’

M-csf F: 5’-CTGACACAGGCCATGTGGAG-3’

R: 5’-GAGAGGGTAGTGGTGGATGT-3’

Rankl F: 5’-GCA CAC CTC ACC ATC AAT GCT-3’

R: 5’-GGT ACC AAG AGG ACA GAG TGA CTT TA-3’

Fra-1 F: 5’-GCAGAAACCGAAGAAAGGAG-3’

R: 5’-CCGATTTCTCATCCTCCAAT-3’.

Erα F: 5’- TCCTTCTAGACCCTTCAGTGA-3’

R: 5’- ACATGTCAAAGATCTCCACCATGCC-3’.

Erβ F: 5’- AAAGCCAAGAGAAACGGTGGGCAT-3’

R: 5’- GCCAATCATGTGCACCAGTTCCTT-3’.

Gapdh F: 5’-CCACAGTCCATGCCATCAC-3’

R: 5’-CATACCAGGAAATGAGCTTGAC-3’.

Western blot analysis

The following antibodies were used: p38α MAPK (Cell Signaling, 9212), p-p38MAPK (T180/182) (Cell Signaling, 9211), p53 (c12) (Cell Signaling, 2524), TAK1 (Cell Signaling, 4505), p-TAK1(T184/187) (Cell Signaling, 4531), CREB (Upstate, 05767), p-CREB (Upstate, 6519), p-NF-κB p65 (Ser536) (Cell Signaling, 3031), NF-κB p65 (Cell Signaling, 4767), Estrogen Receptor α (Abcam, ab37438), NF-κB p50/52 (Santa Cruz, sc-8414), p21 (BD, 556430), p16 (Santa Cruz, sc-1207), and β-ACTIN (Santa Cruz, sc-81178).

Chromatin immunoprecipitation (ChIP) primer sequences

Quantitative PCR was carried out to determine the promoter fragments of *Opg* using the following gene-specific primer sets:

0—-101site F:5’-cagaggcaggcagaggcag-3’R :5’-tgtctatgtagctctgcct-3’

-101—-201site F:5’-gtaaatatttcctattagc-3’ R:5’-catttaaaatcatattaaa-3’

-201—-301site F:5’-tttttacttgctgtctcct-3’ R:5’-acattctgagacatagatt-3’

-301—-401site F:5’-catacctttggagggtag -3’ R:5’-gaagtccctaccctaactt-3’

-401—-501site F:5’-aaatttgtcacatcacatc-3’ R:5’-cttgagctagaagtgcaga-3’

-501—-601site F:5’-acaccttgcctagggaatg-3’ R:5’-cagaattggcctgtgggtc-3’

-601—-701site F:5’-tgtagataatcaatctctc-3’ R:5’-aaacatttttctcaaaatg-3’

-701—-801site F:5’-tcagctaatatcccagaca-3’ R:5’-acttaccatccaaataaac-3’

-801—-901site F:5’-gttgttatcacactgttgt-3’ R:5’-gttcactccatcaagacat-3’

-901—-1001site F:5’-tactttgaactcatgatag-3’ R:5’-tagtgagatgtctcctgag-3’

-1001—-1201siteF:5’-acccagctcctgatagaga -3’ R:5’-tctcaagtcagctgtaggt-3’

-1201—-1301siteF:5’-gttgcctatggcatcttgg-3’ R:5’-gatttgcaaaataaggttc-3’

-1301—-1401siteF:5’-tttaaacgtgccaacagca-3’ R:5’-ttgttggctccttagagtc-3’

-1401—-1501siteF:5’-ccctttatgaaagaggatg-3’ R:5’-tcagaagctagggagaacc-3’

-1501—-1601siteF:5’-caacccaggtaaatatgag-3’ R:5’-attgtcctgaaaaacgact-3’

-1601—-1701siteF: 5’-gccatccctacgcgagagg-3’R:5’-ctttctgggagaaggctga-3’

-1701—-1801siteF:5’-ggtacagtgactgagacat-3’ R:5’-gtacacttgggggagccgc-3’

-1801—-1901siteF:5’-tcagcctctcaccacagg-3’ R:5’-aagaacaaggcagcagctg-3’

-1901—-2001siteF:5’-cagctcagcggtggctttc-3’ R:5’-gcgcggaggcgtgggacaa-3’